WITTECK DEVELOPMENT INC.

Open File Report 88-22

MINERALOGY OF METALLURGICAL PRODUCTS FROM LAKE GEORGE ANTIMONY MINE DURHAM RESOURCES INC. PRINCE WILLIAM, N.B. (Project 5273)

by

J.G. Davison
Head, Mineralogical Services
Witteck Development Inc.

Canada-New Brunswick Mineral Development Agreement
Entente Canada-Nouveau-Brunswick L'Exploitation Minérale

Natural Resources and Energy New Brunswick
Ressources Naturelles et Énergie Nouveau-Brunswick
Energy, Mines and Resources Canada
Énergie, Mines et Ressources Canada

Price $4.75

89-01297/

This report has been prepared for:

Minerals and Energy Division
Department of Natural Resources and Energy
New Brunswick

Hon. Morris Green, Minister

1988

MINERALOGY OF METALLURGICAL PRODUCTS FROM LAKE GEORGE ANTIMONY MINE DURHAM RESOURCES INC. PRINCE WILLIAM, N.B. (Project 5273)

This project was funded under the Canada-New Brunswick Mineral Development Agreement, a subsidiary agreement under the Economic and Regional Development Agreement.

Copies available by contacting:

Minerals and Energy Division
Department of Natural Resources and Energy
P. O. Box 6000, Fredericton
New Brunswick E3B 5H1

1988

Report No.: Open File Report 88-22

Author: J.G. Davison, Witteck Development Inc.

Catalogue No.: ISSN 0712-4562

This report should be referenced in the following manner:

DAVISON, J.G. 1988. Mineralogy of metallurgical products from Lake George antimony mine, Durham Resources Inc., Prince William, N.B. New Brunswick Department of Natural Resources and Energy, Minerals and Energy Division, Open File Report 88-22, 89 p.

WITTECK DEVELOPMENT INC.
2640 South Sheridan Way, Mississauga, Ontario, Canada L5J 2M4
Telephone: (416) 823-7381 Telex: 06-982328

MINERALOGY OF METALLURGICAL PRODUCTS FROM LAKE GEORGE ANTIMONY MINE DURHAM RESOURCES INC. PRINCE WILLIAM, N.B.

PROJECT NO. 5273

for

NEW BRUNSWICK DEPARTMENT OF NATURAL RESOURCES AND ENERGY
MINERALS AND ENERGY DIVISION
P.O. BOX 6000
FREDERICTON, NEW BRUNSWICK
E3B 5H1

May 20, 1987

J. G. Davison
Head, Mineralogical Services

1036A

TABLE OF CONTENTS

		Page
1.0	INTRODUCTION	1
2.0	PROCEDURES	2
	2.1 Sample Preparation	2
	2.2 Sample Examination	4
3.0	RESULTS	6
	3.1 Coarse Grind Products	6
	3.2 Fine Grind Products	22
	3.3 Ultrafine Grind Products	32
4.0	DISCUSSION	38
5.0	CONCLUSIONS	46
6.0	RECOMMENDATIONS FOR FURTHER WORK	48
APPENDIX I	Photomicrographs	49

NOTE: Colour photomicrographs are available for viewing at the Minerals and Energy Division office, Fredericton, N.B.

LIST OF FIGURES

		Page
FIGURE 1	Cumulative Liberation Yield - Coarse Feed	11
FIGURE 2	Liberation and Effective Liberation (Recovery) of Native Antimony in Feed Product	15
FIGURE 3	Cumulative Liberation Yield - Coarse Concentrate	16
FIGURE 4	Cumulative Liberation Yield - Coarse Tailings	21
FIGURE 5	Cumulative Liberation Yield - Fine Feed	28
FIGURE 6	Cumulative Liberation Yield - Fine Concentrate	30
FIGURE 7	Cumulative Liberation Yield - Fine Tailings	31
FIGURE 8	Cumulative Liberation Yield - Ultrafine Feed	34
FIGURE 9	Cumulative Liberation Yield - Ultrafine Concentrate	35
FIGURE 10	Cumulative Liberation Yield - Ultrafine Tailings	37
FIGURE 11	Frequency Diagram Indicating Quantity of Liberated (Free) Stibnite (Berthierite) in Three Feed Products	39
FIGURE 12	Antimony Recovery to Flotation Concentrate	41

LIST OF TABLES

		Page
TABLE 1	Sample Descriptions	3
TABLE 2	Mineral Ratios by Product Type	12
TABLE 3	Mineral Liberation by Product Type	13
TABLE 4	Binary and Polymineralic Associations	14
TABLE 5	Stibnite-Berthierite Liberation and Mineral Content in Binary Particles	18
TABLE 6	Native Antimony Liberation and Mineral Content in Binary Particles	19
TABLE 7	Antimony Assays and Recovery to Flotation Concentrate	23
TABLE 8	Mineral Assays by Product Type (by weight)	24
TABLE 9	Antimony Contents in Minerals	25
TABLE 10	Grade, Recovery, Weight Percent in Flotation Concentrate	26

1.0 INTRODUCTION

At the request of Mr. George Sproul of New Brunswick Natural Resources and Energy, Minerals and Energy Division, nine samples of metallurgical products from the Lake George antimony mine, controlled by Durham Resources Inc., were submitted to Witteck Development Inc. for mineralogical investigation.

The samples represented froth flotation feed, concentrate and tailings products comprising coarse, fine and ultrafine grinds estimated at plus 75 microns, 25 to 75 microns and minus 25 microns, respectively.

Of particular importance in this study was the quantitative mineralogy of the antimony minerals. As such, the distribution of antimony and antimony minerals between products and the degree of liberation of the antimony minerals from sulphide and non-sulphide gangue were examined in detail for each mill product. Data presentations in tables, histograms and semi-log plots were utilized to summarize the results in a useful format. In addition, photomicrographs were supplied to visually quantify and qualify mineralogical data.

2.0 PROCEDURES

2.1 Sample Preparation

Nine samples, representing metallurgical products from bench scale grinding and flotation testwork, were received. The samples comprised flotation feed, concentrates and tailings from three different grinds, specifically plus 75 micron, 25 to 75 micron and minus 25 micron.

Each of the nine samples were thoroughly homogenized by rolling and were subsequently split into two charges. One charge from each of the nine samples was rolled and split into two halves. Each half sample was prepared into 25 mm diameter polished mounts (cold setting epoxy-acrylic). Therefore, two polished mounts were prepared for each mill product.

The remaining products were submitted for antimony analyses. The samples were prepared by acid dissolution techniques and analyzed by atomic absorption spectrophotometer. All results were reported in weight percent antimony (Sb%).

The sample numbers, polished mounts and product types are given in Table 1.

Table 1

SAMPLE DESCRIPTION

Sample #	Sample Type	Polished Section #
87-242	Ultrafine Feed	5273-1 5273-2
87-245	Ultrafine Tailings	5273-7 5273-8
87-248	Ultrafine Concentrate	5273-13 5273-14
87-243	Fine Feed	5273-3 5273-4
87-246	Fine Tailings	5273-9 5273-10
87-249	Fine Concentrate	5273-15 5273-16
87-244	Coarse Feed	5273-5 5273-6
87-247	Coarse Tailings	5273-11 5273-12
87-250	Coarse Concentrate	5273-17 5273-18

2.2 Sample Preparation

Each polished mount was examined under reflected light using a Leitz polarizing microscope with magnifications of 50x, 100x, 200x, 500x and 1250x, the latter using oil immersion. Each sample was scanned along parallel traverses at 300 to 500 micron intervals for mineral textures, mineral types and descriptive information. For quantitative mineralogy, representative scans were conducted at 500 to 1000 micron intervals. The following types of information were accumulated by microscopic field counting of areas of the grain surfaces occupied by liberated minerals and complex polymineralic particles.

1. Modal analysis of valuable antimony minerals.

2. Proportion of liberated versus unliberated valuable minerals.

3. Proportion of unliberated valuable mineral and diluent mineral(s).

4. Average size and range of distribution for each mineral of interest.

As such, it should be noted that the mineralogical analyses were conducted on the overall mill product, rather than Tyler screen fractions of each product. The proportion of free and unliberated mineral grains were calculated to assess the performance of the grinding and flotation process. In addition, the unliberated valuable minerals were observed to assess potential liberation by grind modifications. Again, it should be noted that subjacent gangue, whether sulphide or non-sulphide, may be in middling associations with liberated grains and also that slicing effects may account for variations in mineral contents and size distribution.

To support the quantitative mineralogical investigation, data presentation will utilize semi-log plots, histograms, bar graphs and tables, the latter describing binary and polymineralic associations of unliberated antimony minerals. Also, photomicrographs of each product are used to illustrate mineralogy, textures of liberated and unliberated particles, and an assessment of the degree of liberation.

Chemical data from the antimony analyses were used to calculate mineral recoveries to flotation concentrates, mineral assays (weight percent) within specific products, and to assess concentrate grades and mineral content. Mineral assays, by volume, were not calculated for each product since specific gravity factors were not calculated for the unwanted diluent phases within each product.

3.0 RESULTS

3.1 Coarse Grind Products

The valuable mineral assemblage was comprised primarily of stibnite with lesser berthierite and native antimony and trace amounts of tetrahedrite-tennantite. The gangue mineralogy consisted of sulphide and non-sulphide phases. The latter were tentatively identified as silicates with lesser carbonate while the sulphide phases comprised pyrite and pyrrhotite with lesser chalcopyrite and arsenopyrite. Examples of the mineralogical and textural relationships for the mill products are given in Appendix I.

The stibnite occurred as strongly idiomorphic to xenomorphic angular, prismatic to equant crystals. Grain boundaries ranged from highly ragged fragments to smooth euhedra. Coarse particles commonly exhibited undulatory sector twinning and wedge polysynthetic pressure twins. Bent or folded, ribbon to bleb lamellar twins are also common. The fine particles of stibnite commonly formed crystal aggregates exhibiting equant granular crystals with well developed triple junctions or subequant prisms interlocking with granular crystals. Subgrain development occurred adjacent to coarse stibnite crystals. Brecciation and fragmentation of stibnite were present in few grains.

The coarse stibnite ranged in size from less than 50 microns to a maximum dimension of 400 microns with an average of approximately 125 microns. The fine equigranular stibnite aggregates which ranged up to 300 microns typically contained 2 to 40 micron individual equant to prismatic crystals.

In addition to liberated particles, the stibnite formed binary associations with pyrrhotite, native antimony, silicate gangue and chalcopyrite. Due to the optical similarity of stibnite and berthierite, the quantitative mineralogical data is based on the combination of these two phases pending further scanning electron microscopy and x-ray analysis.

The stibnite occurred both as binary middling (or polymineralic middling) to encapsulated crystals within the silicate gangue commonly associated with one or several sulphide minerals. Within silicate gangue, the stibnite occurred as encapsulated coarse crystal aggregates up to 140 microns ranging down to less than two microns. The unliberated stibnite formed idiomorphic prisms or needles randomly oriented within the gangue and ranged in size up to 2 x 110 microns, whereas equant prisms commonly ranged from 10 to 50 microns in diameter. The silicates, exhibiting multiple compositional types, may occur as precursors to stibnite, displayed by the stibnite interstitial cementation and also by stibnite disseminated within gangue phase #1 interstitial to gangue phase #2. The interstitial stibnite exhibited both idiomorphic passive crystallization and ragged replacement mineralization.

Stibnite-pyrrhotite binary particles suggest that pyrrhotite postdates and locally replaced stibnite by pseudomorphic corrosion. Interstitial pyrrhotite cement formed around stibnite prisms and locally relicts of stibnite are observed in strongly pseudomorphic pyrrhotite grains. The interstitial intergrowths may display myrmekitic textures.

Stibnite may locally postdate the pyrrhotite as subidiomorphic pyrrhotite are overgrown by a matrix of stibnite plus/minus native antimony.

Binary particles of stibnite (and berthierite) with pyrite or pyrite-arsenopyrite intergrowths were observed. The pyrite, which formed idiomorphic to xenomorphic crystals, exhibited overgrowth cementation by the stibnite. The fracture and interstice filling stibnite ranged from less than one micron to ten microns in width. Middling binary particles of stibnite-berthierite with sulphides present, though not common, are observed.

Stibnite also occurred as fine crystals in polymineralic associations, both middling and locked with chalcopyrite-pyrrhotite-antimony-silicate gangue. In most examples, the stibnite formed idiomorphic needles locally overgrown by sulphides and/or native antimony and encapsulated or held by gangue silicates. The silicate minerals enclosing stibnite ranged up to 380 microns in diameter and averaged 140 microns.

Native antimony typically occurred as 2 to 20 micron, equant to lenticular, idiomorphic to xenomorphic, crystals. The individual crystals commonly exhibit smooth grain boundaries and average approximately 8-10 microns in diameter. Maximum size of equant, polygonal grains of antimony was 105 microns. Aggregates of minute native antimony crystals were predominant. Liberated crystal aggregates had maximum diameters of approximately 105 microns with an average of 60 to 70 microns. Unliberated native antimony were typically smaller with a maximum diameter of 70 microns and an average size of less than 40-45 microns. In addition to free particles, the native antimony formed several mineral associations. These included binary associations with stibnite or pyrrhotite and binary to polymineralic associations with silicate or carbonate gangue and sulphides.

Middling and binary associations with stibnite were common. The antimony formed coarse myrmekitic intergrowths with sitbnite, with angular lenticular crystal aggregates ranging from 5 to 50 microns. The antimony also occurred as encapsulated grains within stibnite crystals or as minute interstitial cementation of porous stibnite aggregates. The stibnite locally occurred as middling binaries with antimony such that both minerals have maximum surface exposure.

In addition to stibnite, the antimony commonly formed binary associations with pyrrhotite. The range of mineral content vary from less than 5% antimony to greater than 95% antimony. The pyrrhotite formed interstitial to the earlier antimony and clearly exhibited both passive cementation and fracture fill to corrosion replacement textures after the native antimony. As such, the association displays idiomorphic to strongly xenomorphic, locally dissmeninated crystals and crystal relicts of native antimony within the pyrrhotite cement. Pyrrhotite binaries with antimony exhibit excellent to very poor liberation characteristics as the pyrrhotite fracture fill and disseminated crystal relicts of antimony commonly are less than 2 microns in size. The crystal relicts display ragged, locally brecciated, lobate margins due to pyrrhotite replacement.

The native antimony also occurred as binary (to ternary) associations with silicate gangue (and stibnite). Minute crystals of antimony ranging up to 35 microns are encapsulated by the silicate matrix. In many particles, the antimony is accompanied by idiomorphic prismatic to equant stibnite and, less commonly, with chalcopyrite, arsenopyrite and pyrite. The native antimony minerals content within the silicate particles was generally less than 20%. Although stibnite and antimony exhibited locked associations with a later silicate matrix, the

stibnite and antimony also form interstitial to silicate phases in passive cementation and cleavage or fracture controlled replacement. Binary particles of coarse antimony with silicate gangue are less common. The antimony exhibited middling exposed associations with particle sizes ranging up to 130 microns.

For each of the three mill products, feed, flotation concentrate and tailings, the mineral liberation was calculated for the antimony-bearing minerals. As noted, the stibnite-berthierite was estimated at approximately 95:5 for the feed and concentrates based on particle coloration and morphology. In addition, due to the minute amount of tetrahedrite observed, and its low antimony content relative to the stibnite (berthierite) and antimony, it will not be included in the liberation calculations. However, its textural and liberation character will be noted.

The mineral ratios for the coarse mill products are given in Table 2. Surface area determinations of the mineral liberation in the coarse feed material (see Table 3) indicated that liberated stibnite (plus berthierite) comprised 62.9% of the occurrences, whereas liberation of native antimony was only 11%. The liberated stibnite averaged between 100 to 125 microns in diameter, whereas the binary associations averaged between 35-40 microns. Binary unliberated stibnite ranged up to 70 by 180 microns and were associated primarily with silicate gangue (Table 4). Encapsulated stibnite typically ranged from an average of 10 microns to a maximum of 25 microns, though coarse crystals occurred in silicate gangue up to 400 microns in diameter. Stibnite (berthierite) liberation and the mineral contents of the binary particles are given in Table 5. Cumulative liberation yield diagrams (Figure 1) indicate the

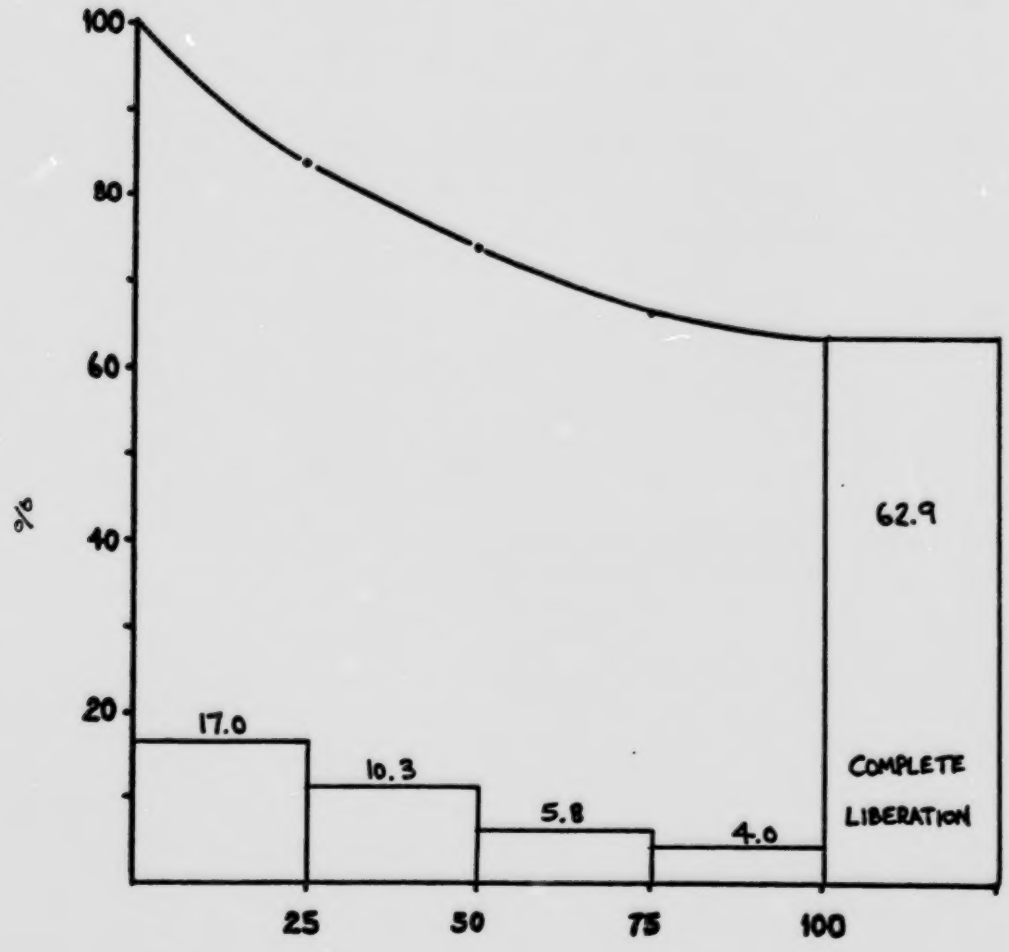

FIGURE 1. Cumulative Liberation Yield - Coarse Feed

Table 2

MINERAL RATIOS BY PRODUCT TYPE

Product	Grind	Coarse	Fine	Ultrafine
Feed	Stibnite*	90.5	90.1	90.5
	Antimony	4.0	4.4	4.0
	Berthierite	5.0	5.0	5.0
	Tetrahedrite	0.5	0.5	0.5
Concentrate	Stibnite	92.2	93.3	92.8
	Antimony	2.2	1.0	1.5
	Berthierite	5.1	5.2	5.2
	Tetrahedrite	0.5	0.5	0.5
Tailings	Stibnite	92.5	89.2	92.5
	Antimony	1.7	6.4	1.9
	Berthierite	5.3	3.9	5.1
	Tetrahedrite	0.5	0.5	0.5

*Stibnite - berthierite ratio estimated from particle coloration and morphology

Table 3

MINERAL LIBERATION BY PRODUCT TYPE
(VOLUME %, FREQUENCY %/VOLUME %)

Mineral: Stibnite

Grind / Product	Coarse	Fine	Ultrafine
Feed	62.9	92.0	97.0
Flotation Concentrate	88.0	98.7	99.5
Flotation Tailings	11.7	48.3	70.5/89.0

Mineral: Native Antimony

Product			
Feed	11.0	36.6	62.3
Flotation Concentrate			
-50 micron	5.1	13.0	56.5/72.8
+50 micron	31.68	45.2	-
Flotation Tailings	0.0	22.0	0.0

1036A

Table 4

BINARY AND POLYMINERALIC ASSOCIATIONS

Grind/Product	Mineral Association					
	Stibnite/Berthierite			Native Antimony		
	Sulphide	Sb	Other	Sulphide	Stb	Other
Coarse Feed	2.5	2.2	95.3	18.2	37.9	43.9
Concentrate	4.2	10.5	85.3	4.8/34.7	72.8/17.8	22.4/47.5
Tailing	-	-	100.0	8.1	16.1	75.8
Fine Feed	1.0	3.3	95.7	10.4	40.8	48.8
Concentrate	3.8	27.7	68.5	17.5/43.6	66.5/49.1	16.0/7.2
Tailing	-	1.7	98.3	-	14.0	86.0
Ultrafine Feed	12.0	10.0	78.0	-	58.8	41.2
Concentrate	16.8	80.3	2.9	37.4	56.1	6.4
Tailing	19.8	3.3	76.9	26.3	3.7	70.0

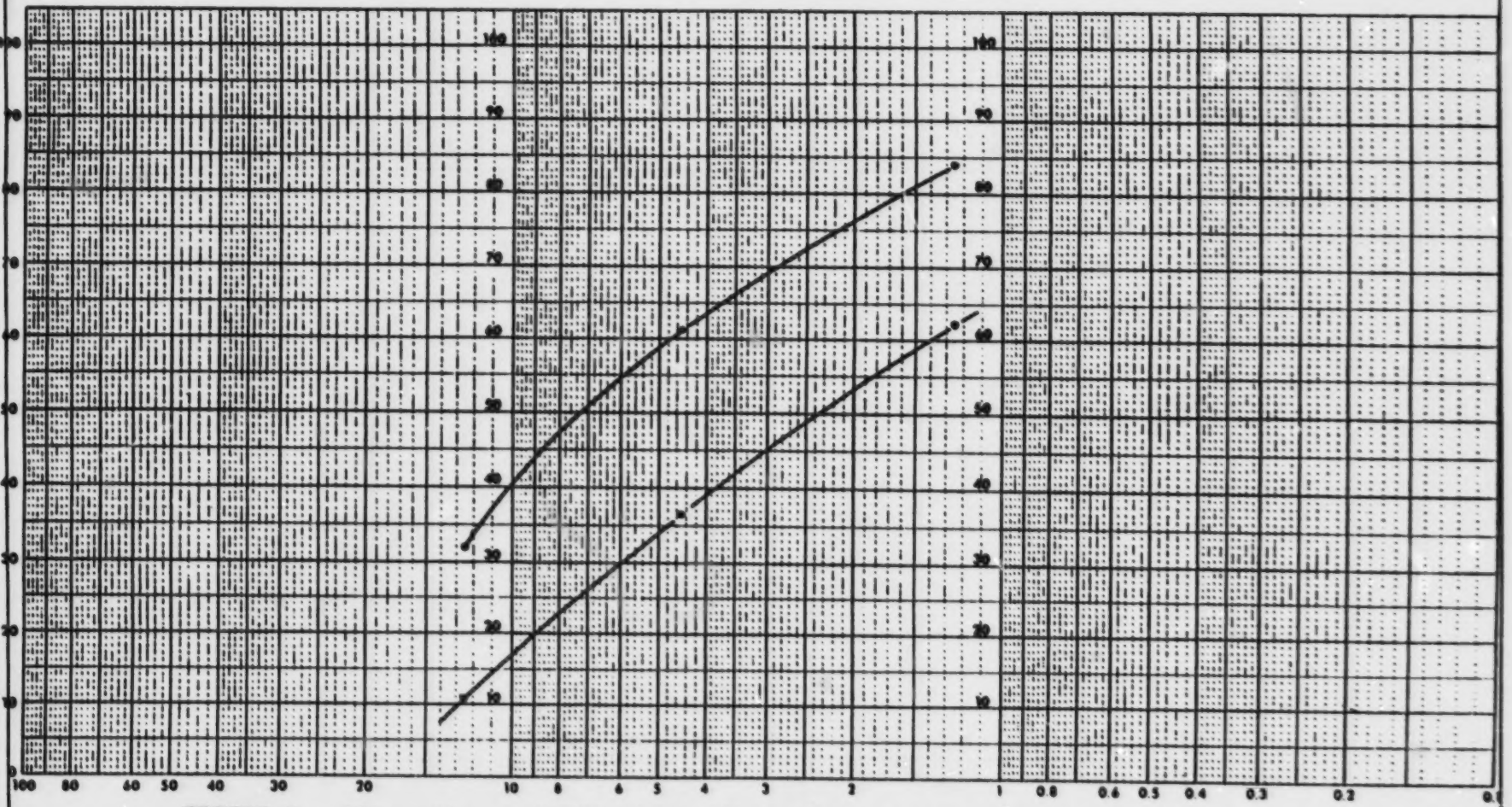

FIGURE 2. Liberation and Effective Liberation of Native Antimony - Feed Products

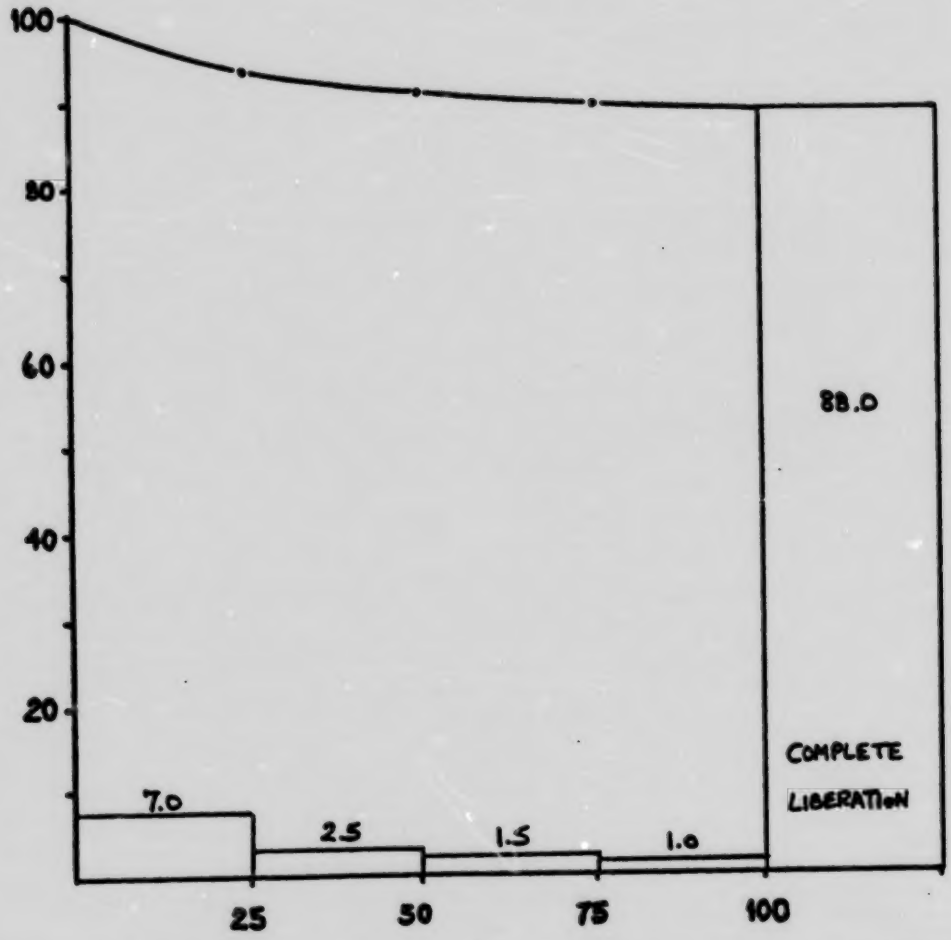

FIGURE 3. Cumulative Liberation Yield - Coarse Concentrate

large proportion of unliberated stibnite and relative distribution by mineral content. The unliberated stibnite (Table 4) was also associated with pyrite, though these occurrences were rare.

Native antimony mineral liberation and the mineral content of its binary particles are displayed in Table 6. Native antimony averaged 10 to 15 microns in diameter with grain aggregates to 75 x 100 microns. Binary associations with stibnite, pyrrhotite and silicate gangue were observed (Table 4). The stibnite-antimony binaries have increased the effective liberation of the native antimony to greater than 32% (see Figure 2). The potential increased liberation of antimony, also indicated by Figure 2, is exhibited by the high percentage of antimony in the mineral content in pyrrhotite or silicate gangue binary associations (see Tables 4 and 6).

In the flotation concentrate, complete liberation of 88% of the stibnite was observed (see Table 3, Figure 3). Mineral ratios are given in Table 2. For native antimony, the liberation was calculated for plus 50 micron and minus 50 micron particles. As such, complete liberation was observed in 5.1% of the minus 50 micron fraction with 31.68% liberated in the plus 50 micron fraction (Table 3). Volume distribution was calculated at 90% plus 50 micron:10% minus 50 micron based on surface area of grains. Recovery of antimony associated in binary particles with stibnite comprised 72.8% of minus 50 micron for overall recovery of 77.9% with an additional 17.8% stibnite-antimony binaries in the plus 50 micron fraction for overall recovery of 50%. Cumulative liberation yields for stibnite (Figure 3) indicate minor potential liberation at finer grinds although the size distribution data suggests excellent liberation potential. Binary diluents in the concentrate product (Table 4) are primarily comprised of pyrrhotite and/or silicate gangue

Table 5

STIBNITE-BERTHIERITE LIBERATION AND MINERAL CONTENT IN BINARY PARTICLES

Product/Grind	Mineral Content (vol %)				
	0-25	25-30	50-75	75-100	Liberated
Coarse Feed	17.0	10.3	5.8	4.0	62.9
Concentrate	7.0	2.5	1.5	1.0	88.0
Tailings	57.1	9.1	15.8	6.3	11.7
Fine Feed	3.9	1.1	1.1	1.9	92.0
Concentrate	0.19	0.27	0.30	0.52	98.7
Tailings	37.7	7.4	4.8	1.8	48.3
Ultrafine Feed	1.8	0.54	0.44	0.23	97.0
Concentrate	0.03	0.05	0.12	0.288	99.5
Tailings	2.38	2.52	3.0	3.1	89.0

Table 6

NATIVE ANTIMONY LIBERATION AND MINERAL CONTENT IN BINARY PARTICLES

Grind/Product	Mineral Content (vol %)				
	0-25	25-50	50-75	75-100	Liberated
Coarse Feed	30.0	18.9	32.4	7.7	11.0
Concentrate	90.3/14.8	4.6/25.4	0/7.64	0/20.3	5.1/31.7
Tailings	69.3	6.5	0	24.2	0
Fine Feed	23.2	8.2	7.3	34.3	36.6
Concentrate	66.5/2.3	13/9.5	4.1/11.9	3.2/30.9	13.0/45.2
Tailings	72.6	0	0	5.4	22.0
Ultrafine Feed	10.4	2.5	1.5	23.3	62.3
Concentrate	0.5	3.2	5.4	18.1	72.8
Tailings	25.9	14.9	25.9	33.3	0.0

with minor chalcopyrite, pyrite and arsenopyrite. Relative percentages of sulphide and non-sulphide diluents are given in Table 4. Cumulative liberation yield of the coarse native antimony (Table 6) indicates extensive upgrading potential of binary particles by further grinding though a high percentage of the antimony is recovered within stibnite-native antimony binaries.

Mineral liberation data of the flotation tailings (Tables 2, 3, 5 and 6) indicated that 11.7% of stibnite was liberated while no occurrences of liberated native antimony were observed. However, liberation yield of the native antimony indicates that 24.2% of the mineral can be readily liberated by minor regrinding (Table 6). Similar data on the stibnite indicates that much of the stibnite (Table 5, Figure 4) occurs at less than 25% mineral grain volumes primarily with silicate gangue or silicate sulphide polymineralic associations. Similarly, the antimony also exhibits a high percentage of low mineral contents within binary associations (Table 4) with only 16% associated with stibnite.

Particle sizes of liberated stibnite averaged 40 to 50 microns with equant aggregates to 200 microns. Middling to encapsulated stibnite ranged up to 290 microns by 80 microns although averaged less than 25 microns. Native antimony averaged less than 10 microns in diameter with a maximum of 40 microns in antimony aggregates. Interstitial stibnite and antimony occurred as binary associations with silicates in particle sizes to 70 x 120 microns.

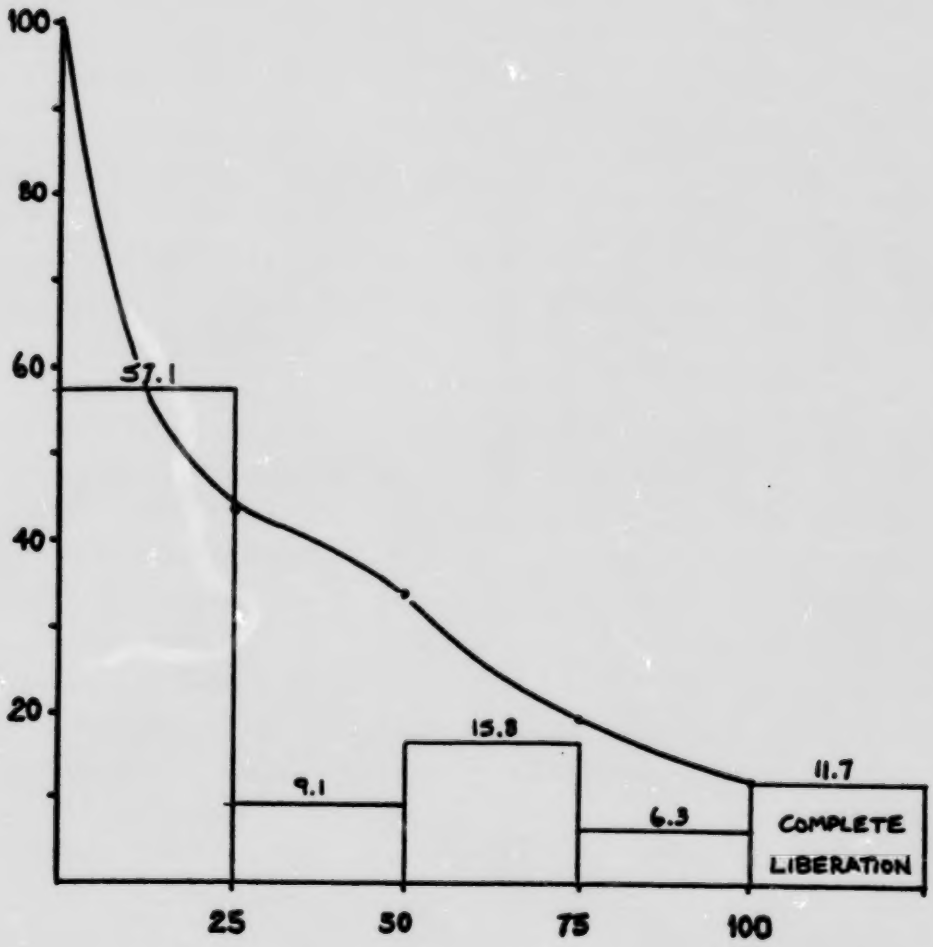

FIGURE 4. Cumulative Liberation Yield - Coarse Tailings

Chemical analyses of the mill products are reported in Table 7. The data indicated antimony metal recovery of 82.1% with a concentrate grade of 61% antimony. Mineral assays were calculated using antimony contents listed in Table 9. The results are given in Table 8. Data indicates that the flotation concentrate contained approximately 85% by weight of antimony mineral with a tailings content of 1.2% mineral. Grade, recovery and flotation concentrate weight calculations are also given in Table 10.

3.2 Fine Grind Products

For each of the mill products, general mineralogical and textural information was summarized in Section 3.1. Only liberation data and chemical analyses will be discussed separately in the following section.

The mineral ratios for each of the mill products are listed in Table 2. Surface area determinations of the mineral liberation in the fine feed exhibit a marked increase from the coarse products with liberated stibnite at 92.0% and native antimony exhibiting 36.6% liberation (Table 3). The liberated stibnite averaged 50-55 microns in diameter with maximum particle sizes of 70 x 150 microns for equant grains and 30 x 205 microns for coarse idiomorphic prisms. Binary associations of stibnite with silicate gangue, sulphides and antimony ranged from 2 to 100 microns in diameter and averaged less than 15 microns with numerous idiomorphic crystals less than 5 microns within silicate gangue. The minute stibnite crystals were typically fully encapsulated by the silicate. Coarser grained stibnite reported as xenomorphic granular aggregates in binary middling to encapsulated associations with both pyrrhotite or silicates. Mineral contents of stibnite with binary and liberated particles

Table 7

ANTIMONY ASSAYS AND RECOVERY TO FLOTATION CONCENTRATE

Grind	Coarse	Fine	Ultrafine
Product			
Feed*	4.82	4.82	4.82
Flotation Concentrate	61.00	58.6*	63.4*
Flotation Tailings	0.869	0.366	0.225
Sb Recovery to Flotation Concentrate	82.10	91.9	95.8
Sb losses to Flotation Tailings	17.90	8.1	4.2

* Average of two analyses

Table 8

MINERAL ASSAYS BY PRODUCT TYPE (by weight)

Product	Mineral	Grind: Coarse	Grind: Fine	Grind: Ultrafine
Feed	Stibnite*		6.09	Average feed values
	Antimony		0.20	
	Berthierite		0.42	
			6.71	
Concentrate	Stibnite	78.55	76.36	82.17
	Antimony	1.34	0.59	0.95
	Berthierite	5.47	5.36	5.79
		85.36	82.31	88.91
Tailings	Stibnite	1.12	0.455	0.291
	Antimony	0.02	0.023	0.004
	Berthierite	0.08	0.025	0.020
		1.22	0.503	0.315

*Stibnite - berthierite ratio estimated from particle coloration and morphology

1036A

Table 9

ANTIMONY CONTENT IN MINERALS

	Vol Wt Ratios	Wt% Sb
Native Antimony (Sb)	121.75/121.75	100.0
Stibnite (Sb_2S_3)	243.5/339.71	71.6
Berthierite ($FeSb_2S_4$)	243.5/427.58	56.9
Tetrahedrite ($Cu_{12}Sb_4S_{13}$)	487/1666.51	29.2

Table 10

GRADE, RECOVERY, WEIGHT PERCENT IN FLOTATION CONCENTRATES

Product	Wt. %	Grade	Recovery
Coarse	6.5	61.00	82.1
Fine	7.5	58.6*	91.9
Ultrafine	7.2	63.4*	95.8

* Average of two analyses

are given in Table 5. Cumulative liberation yield diagrams of the fine feed material indicated a well dispersed array of unliberated stibnite with minor potential for upgrading with minor regrinding. Binary associations with sulphides were not common (approximately 1%) but included middling particles of stibnite plus/minus antimony with pyrite and/or arsenopyrite or chalcopyrite. Distributions of silicate and sulphide binaries are given in Table 4.

Rare occurrences of tetrahedrite formed binary associations with arsenopyrite, pyrite or silicate gangue. The tetrahedrite formed interstitial to the sulphides in xenomorphic aggregates up to 50 microns in diameter. Tetrahedrite was not observed as fully liberated particles and comprised only minor binary middling to encapsulated associations.

Native antimony crystals averaged less than five microns in diameter with maximum crystal size of 50 microns and aggregates to 75 microns. Binary associations with stibnite, gangue silicates and pyrrhotite were observed. The distribution of the binaries are described in Table 4. Approximately 40.8% are associated with stibnite. Effective liberation data indicated that 61% of the native antimony will report to the flotation concentrate. Cumulative liberation yield (Table 6) indicates that a high percentage of coarse binaries with high mineral content can be liberated by minor regrinding.

In the flotation concentrate, complete liberation of 98.7% of the stibnite was observed (Table 3, Figure 6). For native antimony, the liberation was calculated for plus/minus 40 micron particles. The results indicated that 13.5% of the minus 40 micron fraction and 45.2% of the plus 40 micron fraction were completely liberated (Tables 3 and 6). The stibnite averaged

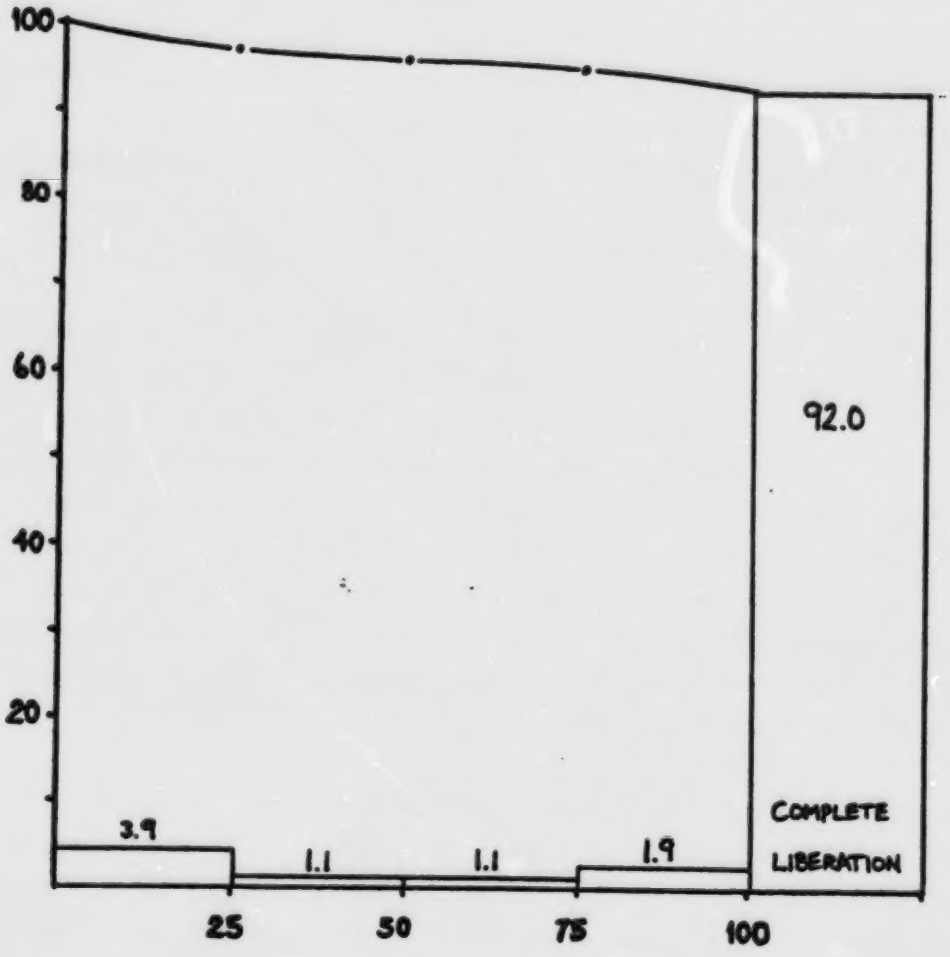

FIGURE 5. Cumulative Liberation Yield - Fine Feed

45-50 microns in diameter with prisms and equant crystals to 160 and 125 microns, respectively. Native antimony averaged less than five microns with a maximum crystal size of 15-20 microns and aggregates to 70 microns. Recovery of native antimony to stibnite comprised 49.1% of the plus 40 micron fraction and 66.5% of the minus 40 micron antimony fraction. Overall recovery estimates for the plus 40 micron antimony increase to 71% with minus 40 micron native antimony to 39.5%. Cumulative liberation yield data (Table 6) indicates a large percentage of high antimony content in binary particles, primarily split between pyrrhotite or stibnite. Silicates are predominant over sulphides in the low mineral content binary particles. Sulphide diluents in the concentrate product also included chalcopyrite, molybdenite, pyrite, and tetrahedrite (see Table 4). Cumulative liberation data for the stibnite indicated minor binary and polymineralic particles due to very high liberation (Table 5, Figure 6). Numerous binary particles indicated by Figure 6 comprise stibnite and native antimony in middling and locked associations with silicate gangue.

Mineral liberation data of the flotation tailings (Tables 2, 3, 5 and 6) indicated that 48% of the stibnite and 22% of the native antimony occurred as liberated particles. Optimized flotation of the liberated particles could enhance recovery to the flotation concentrate. Cumulative liberation data indicated that the binary and polymineralic particles with stibnite are commonly of less than 50% valuable mineral (see Table 5, Figure 7). Similar results were observed for the native antimony such that 72% of the available antimony comprised less than 25% of the binary particle (Table 6). As indicated previously, approximately 40.8% of the antimony binaries will report to the stibnite whereas 10.4% and 48.8% are related to pyrrhotite or silicate binaries, respectively (Table 4).

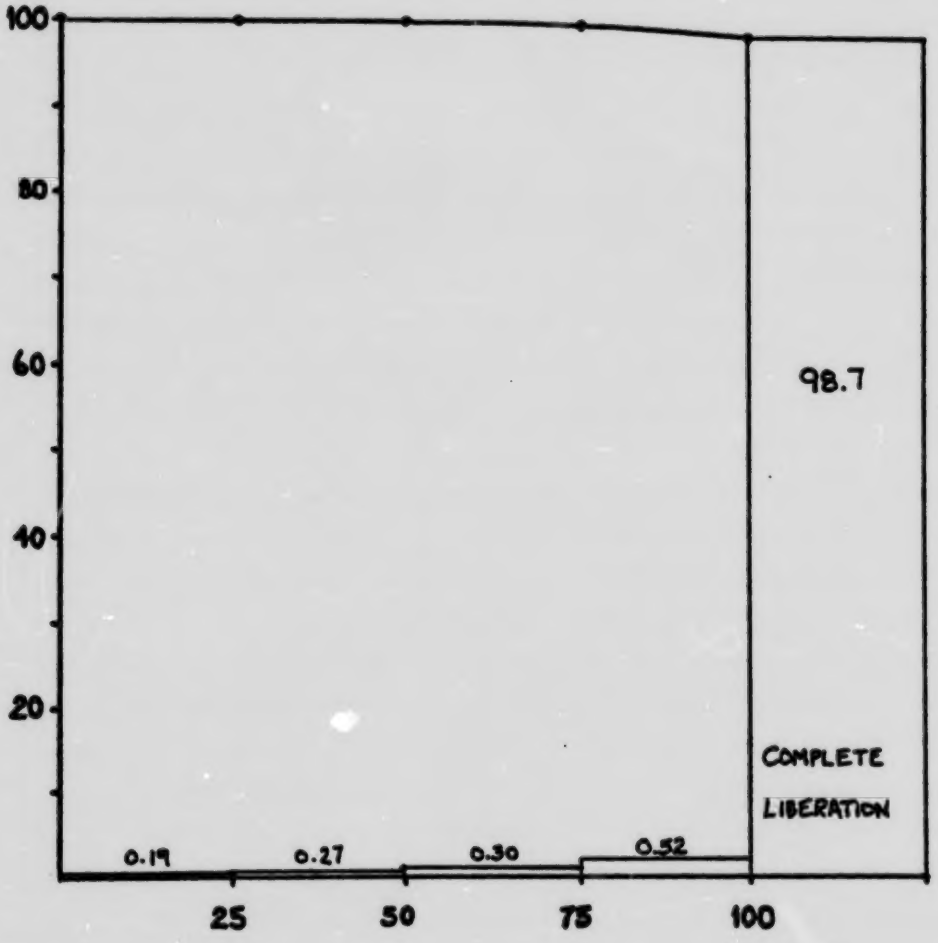

FIGURE 6. Cumulative Liberation Yield - Fine Concentrate

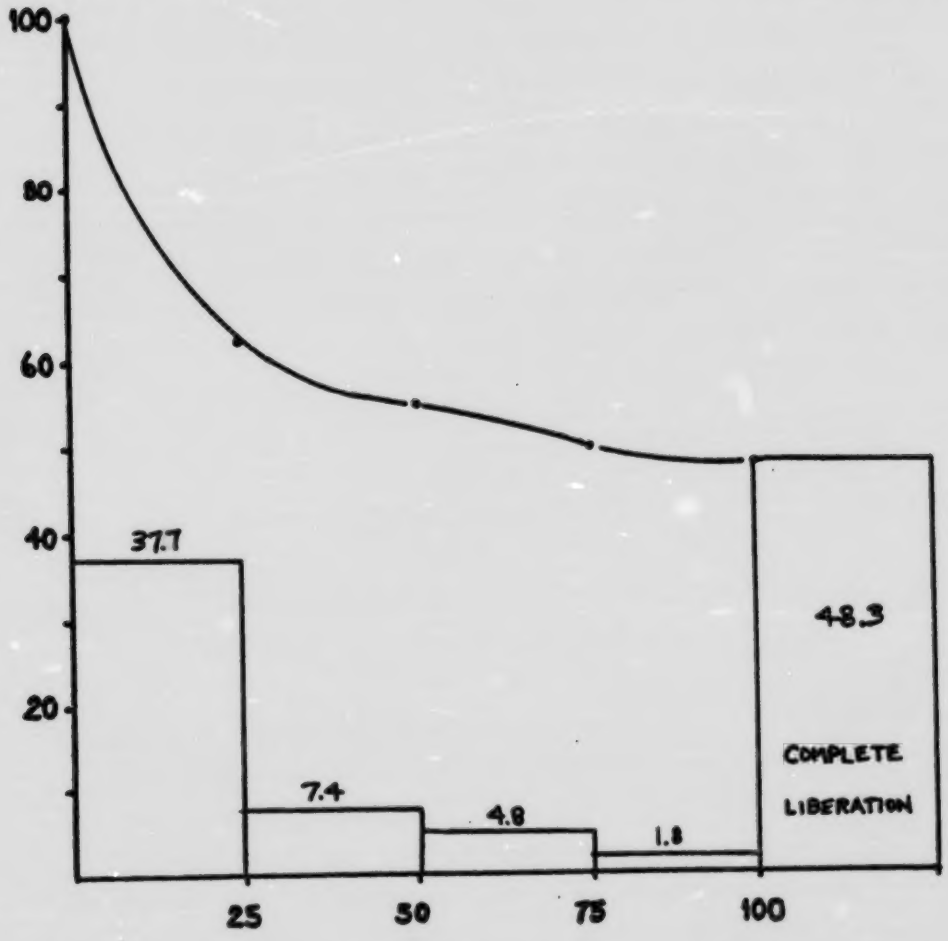

FIGURE 7. Cumulative Liberation Yield - Fine Tailings

Particle sizes of stibnite averaged 15-20 microns with a maximum of 48 microns in binary associations and encapsulated by silicates whereas liberated stibnite averaged 30-35 microns with a maximum of 20x85 microns. Native antimony crystals averaged less than 5 microns with binaries of antimony and pyrrhotite up to 8x60 microns. Antimony aggregates up to 24 x 44 microns were also reported with gangue silicates and/or stibnite.

Chemical analyses of the mill products are reported in Table 7. The data indicated antimony metal recovery to the flotation concentrate of 91.9% at a grade of 58.6% Sb. Mineral assays were calculated using the mineral metal contents indicated in Table 9. The results are shown in Table 8. The data indicated that the flotation concentrate contained approximately 82.3% by weight antimony minerals with a tailings content of 0.5% by weight antimony mineral. The grade recovery and weight percent of concentrate are listed in Table 10.

3.3 Ultrafine Grind Products

For each of the mill products, general mineralogical and textural information was summarized in section 3.1. Only liberation data and chemical analyses will be discussed in this following section.

The mineral ratios for each of the mill products are listed in Table 2. Surface area determinations of the mineral liberation was performed only in the plus 4 micron fraction of the ultrafine products. Routine counting was not conducted on the minus 4 micron particles although qualitative information was obtained. The liberation data, as expected, indicated definite increased mineral liberation, relative to the fine grind. Stibnite liberation in the ultrafine feed was approximately 97%

in the plus 4 micron fraction (Tables 3 and 5) whereas native antimony advanced to a high of 62.3% complete liberation (Tables 3 and 6). The liberated stibnite ranged in size to a maximum of 20x60 microns with an average size of 16 microns. Native antimony occurs as crystals of 1-5 microns in aggregates up to 20x35 microns with an average size of 5-6 microns. Particles are typically xenomorphic angular though, locally, prismatic subidiomorphic stibnite are observed. Cumulative liberation yields (Figure 8) indicated only minor unliberated stibnite. Approximately 87% of the unliberated stibnite (Tables 4 and 5) was associated with silicate binaries while 20% were associated with sulphides, compromising pyrite, pyrrhotite or chalcopyrite. The remaining 2% of the stibnite was associated in binary particles with native antimony.

Cumulative liberation yield data of the native antimony (Tables 4 and 6) reported as minute crystals comprising less than 25% of the host. The host minerals consisted of 42% with silicate gangue and 58% with stibnite. The presence of the binary particles increased the effective liberation (Figure 2) of the native antimony to approximately 84% overall recovery.

In the flotation concentrate, complete liberation of 99.5% of stibnite was observed (see Tables 3, 4 and 5, Figure 9). For native antimony, the liberation was calculated at 72.8% (Table 6). The cumulative liberation yield of the stibnite, given in Figure 9, and Table 5, indicates that additional binary particles are common with greater than 75% valuable mineral content. The binaries are comprised of sulphides including pyrite, chalcopyrite, pyrrhotite, tetrahedrite, and antimony (Table 5). In the latter, approximately 56% of the native antimony binaries are associated with stibnite. Overall effective liberation and recovery of native antimony was increased to 88% with both liberated and binaries with stibnite. The distribution of sulphide and non-sulphide binaries are displayed in Table 6.

1036A

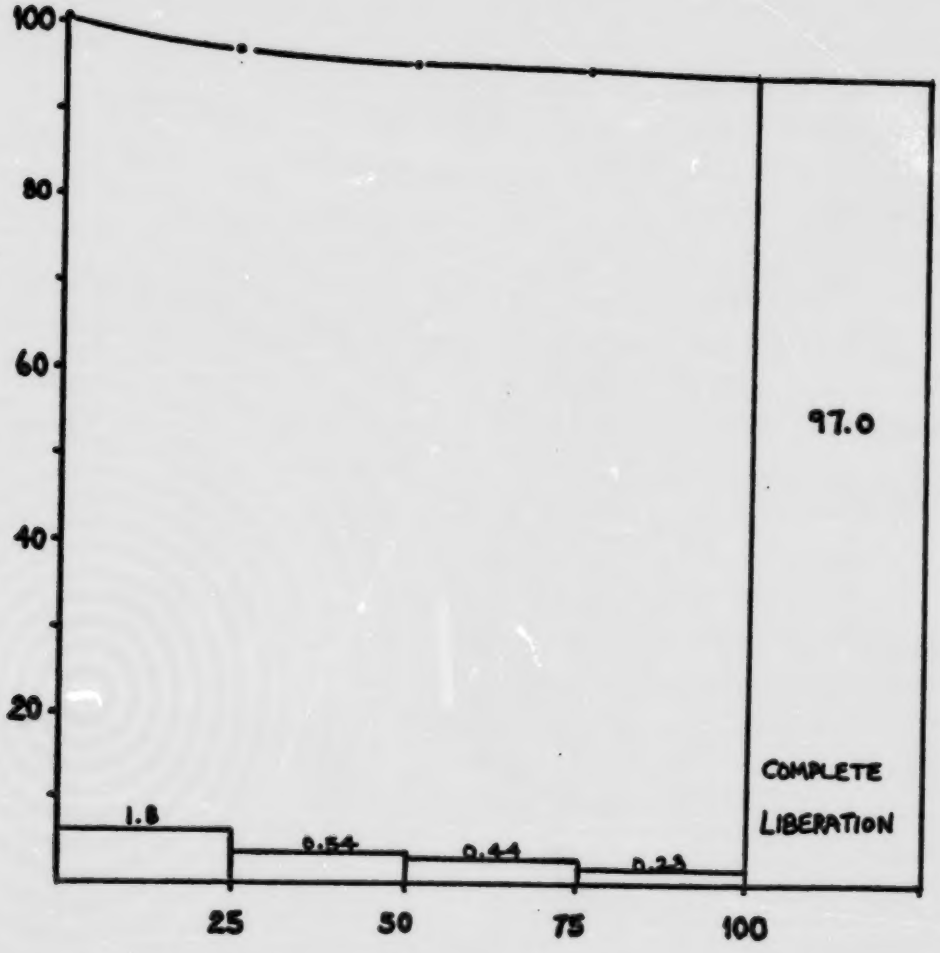

FIGURE 8. Cumulative Liberation Yield - Ultrafine Feed

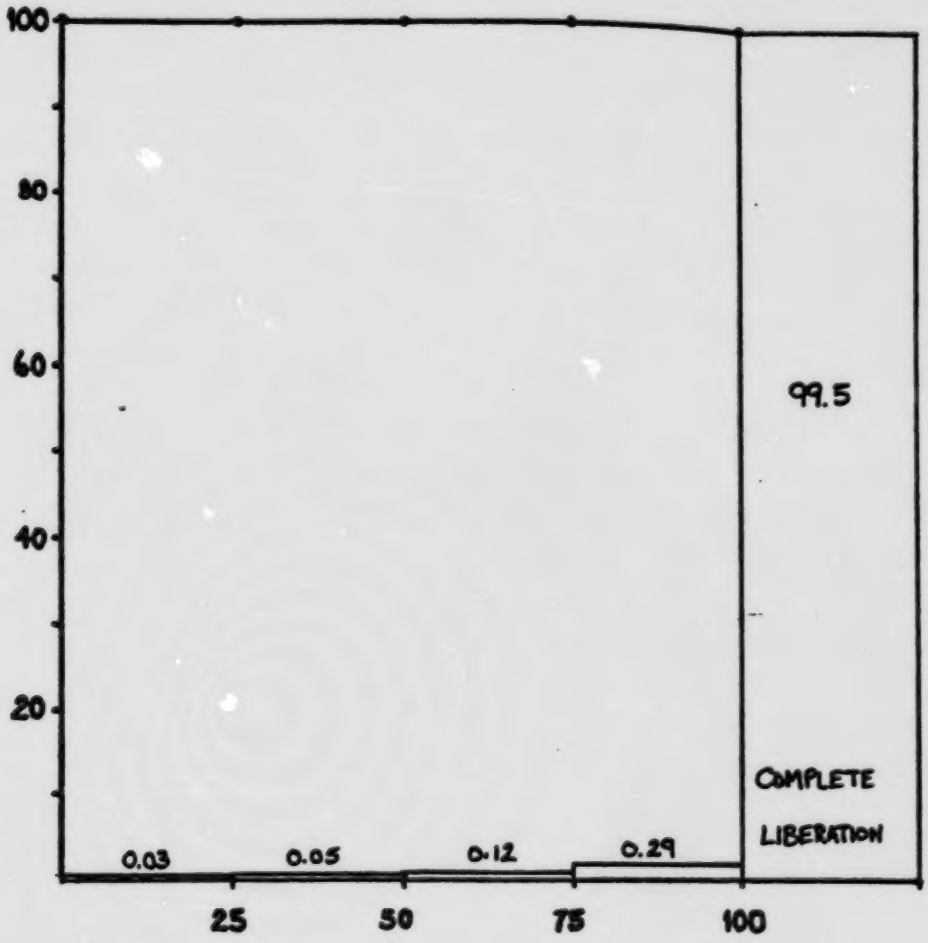

FIGURE 9. Cumulative Liberation Yield - Ultrafine Concentrate

Mineral liberation data on the flotation tailings (Tables 3, 4, 5 and 6) indicated that 89% of the stibnite occurred as liberated particles (Figure 10) while no occurrences of fully liberated native antimony were observed. In addition, only 3.7% of the native antimony occurring in binary particles (Table 4) was associated with stibnite. In that occurrence, native antimony comprised less than 25% of the binary particle. Data on the binary associations of stibnite and antimony, given in Table 4, inidicated that 77% and 50% of the binaries were comprised of antimony minerals with silicate gangue, respectively. Binary associations with pyrite, arsenopyrite and/or tetrahedrite were also noted.

Particle sizes of liberated stibnite averaged 8-10 microns with a maximum of 21x48 microns whereas native antimony had a maximum dimension of 10 microns with an average of 5-6 microns. These figures are restricted to the plus 4 microns fraction particles.

Chemical analyses of the mill products are reported in Table 7. The date indicated antimony metal recovery of 95.8% with a concentrate grade of 63.4% Sb. Mineral assays were calculated using antimony mineral contents given in Table 9. The results are given in Table 8. Data indicates that the flotation concentrate contained 89% by weight of antimony mineral with a tailings content of 0.31% antimony mineral. The grade, recovery, and weight percent of flotation concentrate are displayed in Table 10.

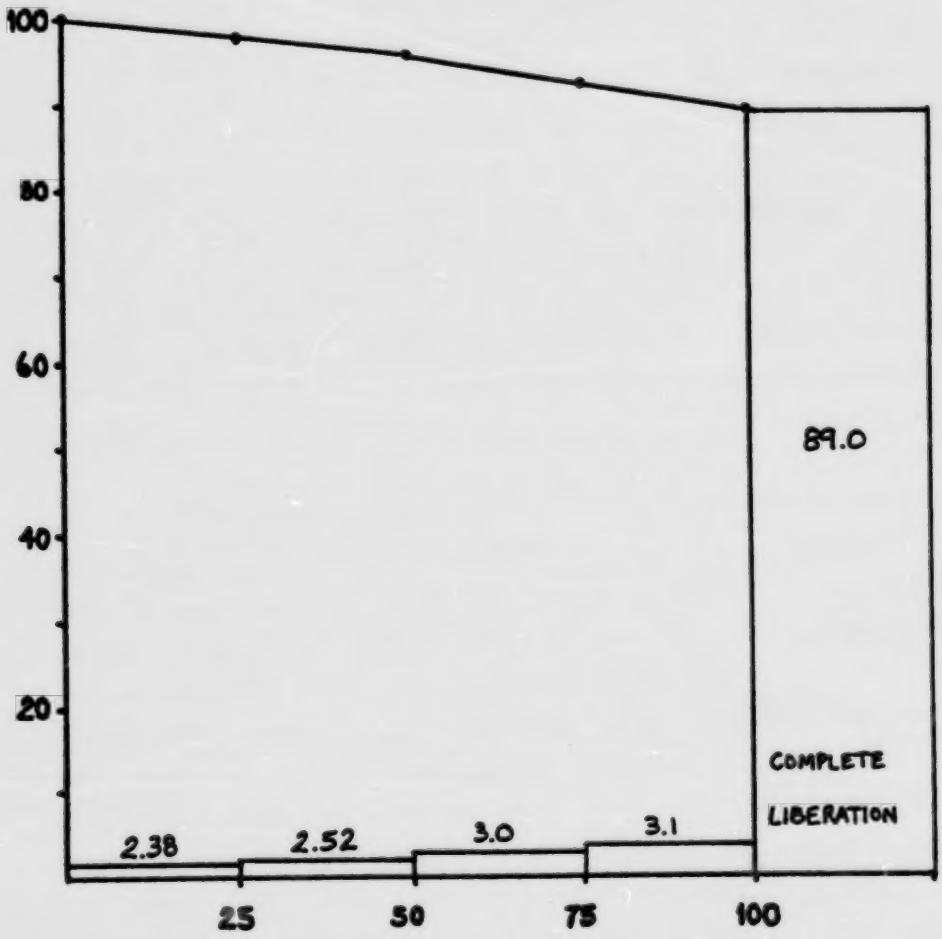

FIGURE 10. Cumulative Liberation Yield - Ultrafine Tailings

4.0 DISCUSSION

Mineral liberation studies were performed on mill products from the Lake George (Durham Resources) antimony mine. The mill feeds, concentrates, and tailings products from a grinding-classification (cyclone) - flotation concentrate circuit represented various grinding times with final products of plus 75 microns, 25 to 75 microns and minus 25 microns. The products were designated as coarse, fine and ultrafine grinds, respectively.

The mineralogical studies identified stibnite (Sb_2S_3) as the major contributor to the valuable mineral assemblage with lesser to trace quantities of berthierite ($FeSb_2S_4$), native antimony (Sb) and tetrahedrite ($Cu_{12}Sb_4S_{13}$). The mineral assemblage of diluent phases was comprised primarily of silicates and carbonates with lesser sulfide minerals consisting of pyrrhotite with minor pyrite, chalcopyrite and arsenopyrite.

Examination of the mill feed products indicated that the antimony minerals occurred as both liberated and unliberated binary to polymineralic associations. Liberation of both stibnite (berthierite) and native antimony, outlined in Table 3, exhibited progressive increases with continued comminution (fine particle sizes) of feed product. Indeed, the native antimony, due to the fine dimensions of the liberated and unliberated particles of less than 40 microns, displayed increased degrees of freedom even at very fine grinds of minus 25 microns. However, stibnite, as shown in Figure 11, displayed a sharp depletion in the rate of liberation, at grinds finer than 45 microns with concomitant small changes in

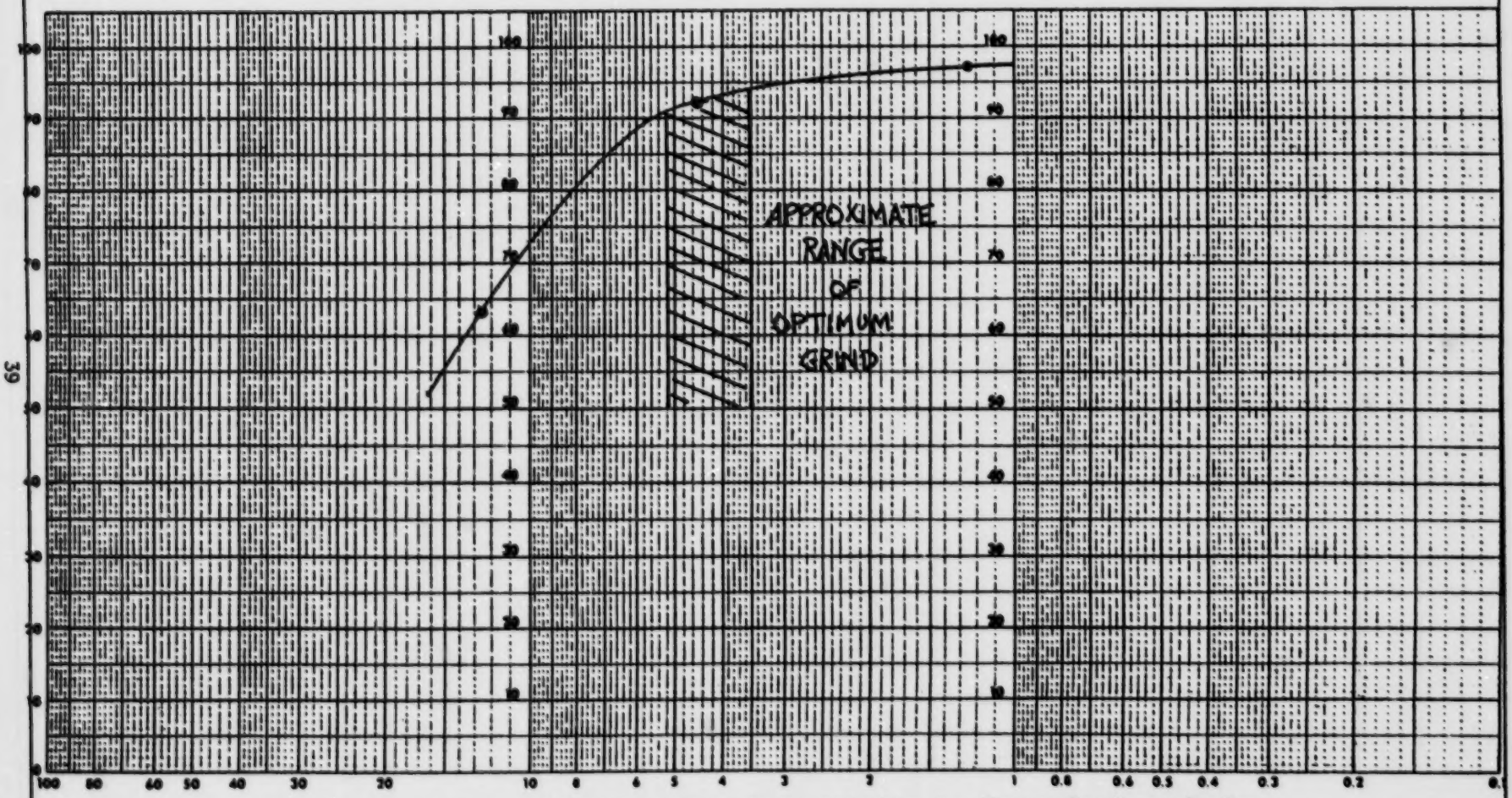

FIGURE 11. Frequency Diagram indicating liberated stibnite in three feed products

overall degree of liberation. Based on this information, the estimated optimum grind for the stibnite-native antimony feed material was approximately 100% minus 52-37 microns. It should be noted that progressive increases in native antimony liberation are volumetrically insignificant to the overall concentrate grade relative to the antimony sulphides.

The extent of the size reduction in the grinding-classification circuit was also evidenced by both the progressive increases in abundances of liberated antimony minerals within the flotation concentrate products (Table 3) and the antimony recovery to the flotation concentrate (Figure 12). The liberated form was clearly the dominant type of occurrence for stibnite (berthierite) while native antimony occurred primarily as binary to ternary particles in concentrate products other than the ultrafine grinds.

Within the flotation tailings products, liberated stibnite exhibited major changes in abundance with increased fineness of grind. In fact, stibnite increased from only 11.7% liberation to 89% liberation (Table 5). The progressive increases in free stibnite losses are partially offset by increased recoveries, thereby dropping the overall contribution of the liberated stibnite in the tailings to the materials balance. However, the abundance of coarse stibnite within binaries of the coarse and fine tailings products indicated that increased liberation can be attained by regrinding of the flotation tailings. Although size distribution data was not available for the individual mill products, the progression of the three grind products were utilized to estimate the optimum conditions.

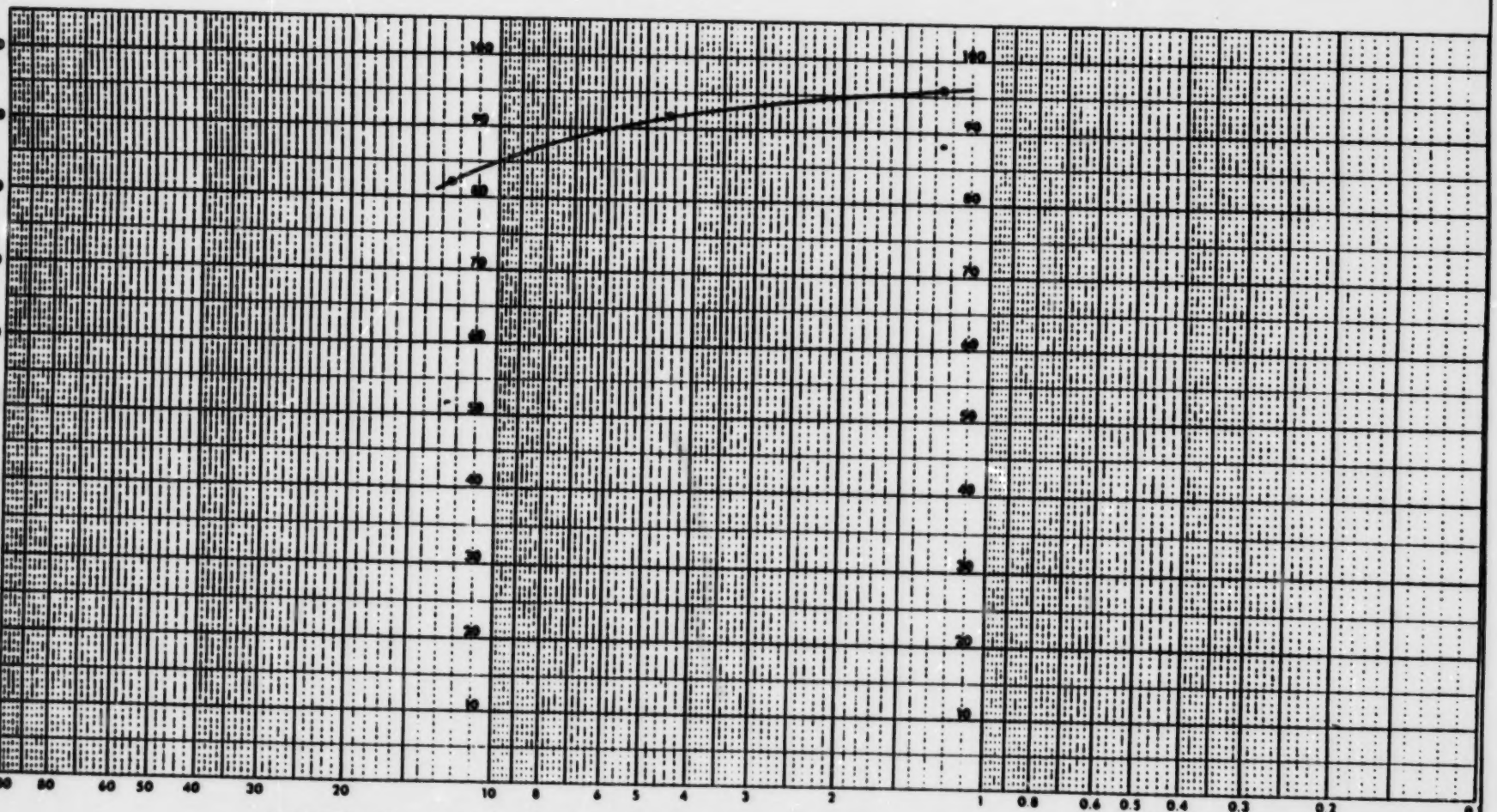

FIGURE 12. Antimony recovery to flotation concentrate

The use of cumulative liberation yield diagrams for each product indicated liberation trends of specific products and changes in overall degrees of liberation with further grinding stages The large slope of the cumulative yield curve in the coarse mill product (Figure 1) suggests that further grinds are required. Rapid flattening of the curves for the fine and particularly for the ultrafine products (Figures 5 and 8) suggest that the optimum grind has been attained since liberation will exhibit only minor increases with protracted comminution.

Similarly, the cumulative yield data for the concentrate products (Figures 3, 6 and 9) suggest that enhanced liberation of stibnite will be achieved, in significant amounts, only by regrinding of coarse to fine product size range. Increased attrition to ultrafine particle sizes is not volumetrically significant to increase the concentrate grade or degree of liberation.

From the data described in Tables 3, 5 and 6 and Figures 4, 7 and 10, it is apparent that the cumulative liberation of stibnite has been achieved by particle size attrition due to the relative depletion of binary and polymineralic associations. However, the increased contents of liberated stibnite, as previously noted, becomes the major contributor to the antimony losses in the flotation tailings.

Relationships between the valuable ore minerals, stibnite and native antimony, versus diluent phases are indicated by Table 7. Within the coarse feed products, binaries and polymineralic associations of stibnite with silicates and minor sulfides were predominant, while binaries of stibnite with sulphides comprise only 2.5% of the unliberated stibnite particles.

Increased grinding to fine products provide similar proportions while the significance of sulphide-stibnite binaries reports a major increase in ultrafine feed products. Recovery of the composite particles of stibnite-native antimony are important to increase overall antimony grades. The data indicated that the proportion of stibnite-native antimony binaries exhibited a strong concentration factor in the flotation products with minor to nil associations of liberated stibnite-antimony binaries within the flotation tailings. With respect to native antimony, the stibnite binaries and binary to composite particles with sulphides, particularly pyrrhotite, are moderately to strongly concentrated while antimony-silicate binaries are rejected to the tailings products. These trends are particularly evident in the ultrafine grinds. Rejection of antimony-sulphide binaries was also achieved in the ultrafine products.

The sulfide-stibnite binaries exhibit preferred residence within the flotation concentrate while silicate binaries are strongly to weakly rejected to the tailings. Rejection of stibnite-silicate binaries exhibited a progressive increase with continued particle comminution. Gangue silicate rejection was particularly strong in the minus 25 micron product. However, several examples of stibnite particles coated by either a silicate or oxide mineral were observed in the ultrafine tailings. Further examination of the tailings products and x-ray analysis would be required to characterize the particle coatings.

The mineralogical analysis have indicated that the major losses of antimony to the flotation tailings are contributed by unliberated stibnite-berthierite and/or native antimony with silicate binaries and to a smaller degree with sulphide

binaries. However, within the coarse grind products, nonliberation of stibnite and antimony comprise 95% of the binary particles (over 35% of available antimony) with losses of liberated stibnite comprising 11% of the tailings. With progressive particle size reduction, the effective liberation and concentrate recovery are increased with depletion of losses due to binary particles. Losses due to liberated stibnite exhibit a proportionate sharp increase from 11-89% of available antimony. With respect to the overall antimony recovery, the liberated stibnite represents 2.1 to 4.45% additional losses strictly due to liberated particles.

Therefore, it is clear that a significant proportion of the antimony losses to the tailings are due to the unusually high proportion of liberated stibnite. From the low recovery and the low proportion of antimony losses to free stibnite in the coarse tailings, it is obvious that finer grinding to reduce the content of binary and polymineralic particles was required to eliminate large quantities of diluent minerals.

To summarize the losses of antimony to the tailings products, the following points are demonstrated.

1. Losses due to binary and polymineralic diluents caused by inadequate comminution of coarse unliberated stibnite-sulphide-silicate complex particles.

2. Losses of liberated stibnite in coarse flotation products may be due to residence time in flotation cells, reagent consumption, or anomalous kinetic or physico-chemical reponses.

3. Losses of unliberated stibnite in fine and ultrafine grinds due to mineral ratios, combined hydrophobicity due to textural character, sliming effects or flotation response due to reagents or residence time.

4. Losses of liberated stibnite in fine and ultrafine grinds potentially due to overgrinding, absence of regrind circuit between flotation banks, absence of flash flotation circuit to skim high percentages of coarsely liberated antimony minerals, or losses due to residence time, sliming, reaction kinetics or depression of extremely fine (less than 10-12 micron) particles with poor flotation characteristics.

5.0 CONCLUSIONS

1. Mineralogical studies of the Lake George (Durham Resources) antimony mine reported the presence of the following valuable antimony minerals.
   - -Stibnite
   - -Berthierite
   - -Native Antimony
   - -Tetrahedrite

2. Mineral liberation studies of the combined mill products for three grind sizes (+75 micron, 25-75 micron, -25 micron) were completed. Calculations were performed on stibnite (berthierite) and native antimony to provide information on grinding-classification and flotation circuit for each mill product.

3. Liberation of stibnite increased from 62.9% to 92% to 97% with finer grinding. Similarly, native antimony exhibited enhanced mineral liberation from 11% to 32% to 62% by fine grinding.

4. Binary and polymineralic particles of stibnite with native antimony, sulphides and silicates were observed in all feed products. Antimony occurred as binary associations with stibnite, silicates and sulphide minerals.

5. Binary associations of stibnite with silicate gangue were predominant whereas antimony occurred in similar proportions with silicates and stibnite and to a lesser degree with sulphide minerals.

6. With increased particle reduction, the proportion of binary and polymineralic associations were decreased in favour of liberated particles.

7. Losses of antimony minerals to the flotation tailings are due to both unliberated and liberated particles of stibnite, and lesser, to native antimony.

8. Losses of antimony in coarse products were primarily due to binary particles although losses of liberated stibnite contributed up to 12% of the antimony content. Losses of antimony in the fine and ultrafine products are primarily due to stibnite-silicate binaries and partially in the ultrafine tailings to liberated stibnite.

9. Losses are attributed to overgrinding of coarsely liberated stibnite, absence of flash flotation for these particles, binary particles associated with silicates in the coarse products due to undergrinding, binary particles in the fine grind due to absence of regrind circuit and kinetic problems within the ultrafine materials particularly with minus 10 micron fraction. The losses of the liberated stibnite in the fine products may be due to reagent consumption, entrainment or sliming effects or incomplete chemical preparation.

10. Grade dilution and low recovery in the coarse grind product was attributed to coarse binary particles of antimony with silicates and carbonates. In addition, sulphide minerals such as pyrite, coated by stibnite, comprised the diluent particles. Similar grades, observed at finer grinds, and enhanced recoveries indicated the depletion of the binary contribution to the concentrate product.

6.0 RECOMMENDATIONS FOR FURTHER WORK

The following investigative studies would be required to fully assess process optimization and mineral behaviour of the antimony mill products.

1. Size fraction analysis utilizing mineral liberation, valuable mineral contents within binary or complex particles, cumulative liberation yield data of mill products representing primary grinding, secondary grinding or regrinding of flotation products, cyclone fractions, rougher, cleaner and scavenger flotation concentrates and tailings products.

2. Size fraction geochemistry to assess weight distribution of specific liberated, binary or complex particles containing valuable antimony minerals.

3. Assessment of various feed types to determine mineralogy, mineral ratios, liberation character, to understand the constant tail grades with highly variable feed grades.

4. Flowsheet assessment to determine viability of unit cell flash flotation of coarse liberated particles in the grinding circuit, regrind circuits, reagent addition points, flotation cell residence time and reaction kinetics, reagent consumptions [eg. $Pb(NO_3)_2$].

5. Evaluation of feeds to determine reasons for grade dilution - low Sb, high Fe possibly due to berthierite, pyrite or ferromagnesian silicates.

6. X-ray examination of fine and ultrafine products to determine type of mineral coatings observed on liberated stibnite particles.

7. X-ray examination to clarify stibnite-berthierite ratios.

APPENDIX I

Photomicrographs

COARSE FEED

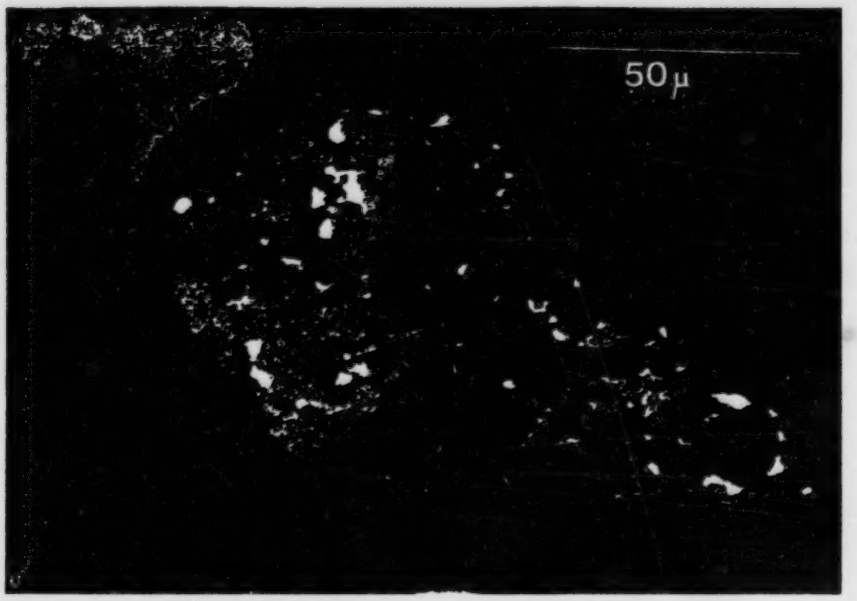

Photograph 1 - 500 X Reflected Light
Liberated polycrystalline aggregate of stibnite contains numerous encapsulated to interstitial xenomorphic crystals of native antimony.

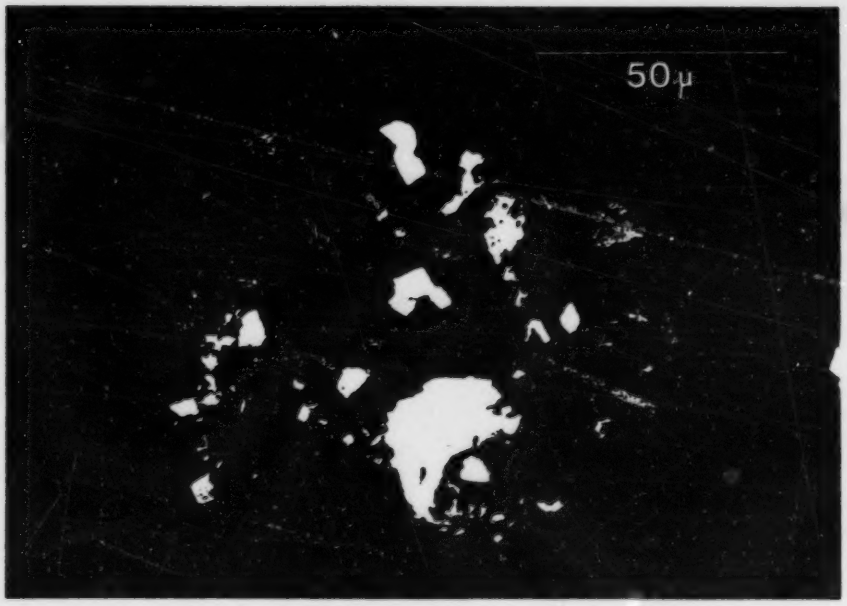

Photograph 2 - 500 X Reflected Light
Example of poor liberation shown by subangular particle of silicate gangue containing numerous equant to prismatic idiomorphic stibnite and idiomorphic to subidiomorphic crystals and aggregates of native antimony. The native antimony typically formed interstitial to stibnite.

Photograph 3 - 500 X Reflected Light
Numerous minute crystals of stibnite and lesser native antimony encapsulated by and interstitial to silicate gangue. Typical example of non-liberation in coarse products.

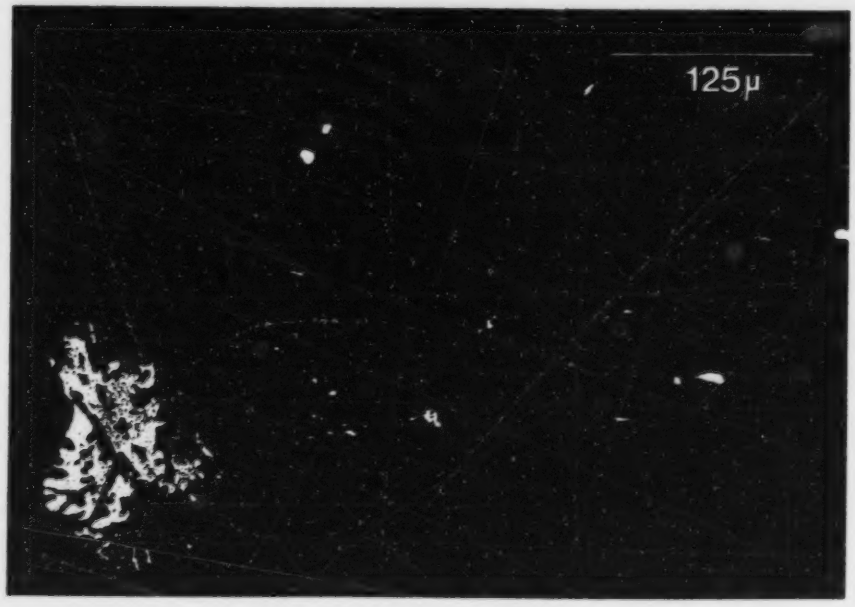

Photograph 4 - 200 X Reflected Light
Coarse to very fine prismatic stibnite and minor native antimony interstitial to and enclosed by two different silicate gangue phases. Stibnite typically formed fine disseminations (see also Photo 3) and less commonly, coarse binary aggregates with silicates.

COARSE CONCENTRATE

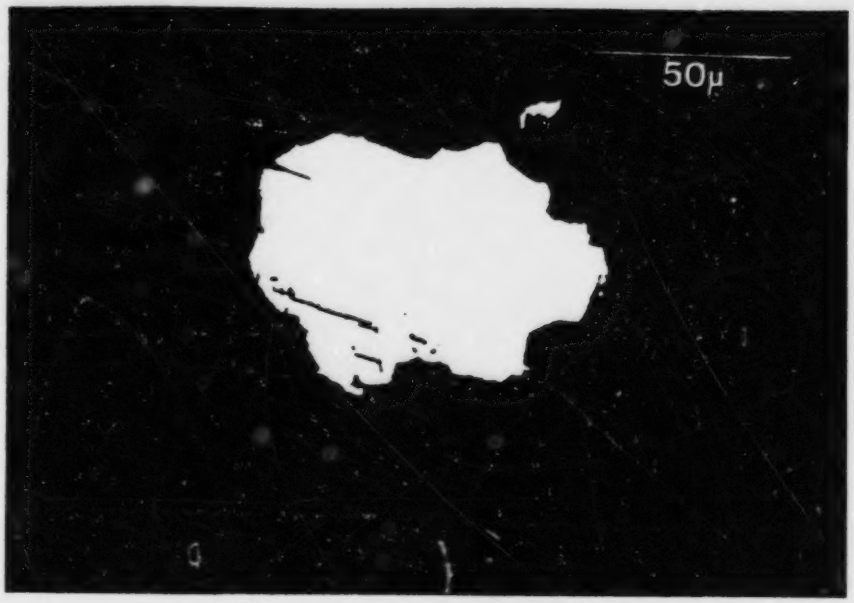

Photograph 5 - 500 X Reflected Light
Coarse xenomorphic native antimony forms binary association with subidiomorphic to xenomorphic stibnite. Minor crystals of silicate gangue are cemented by the stibnite.

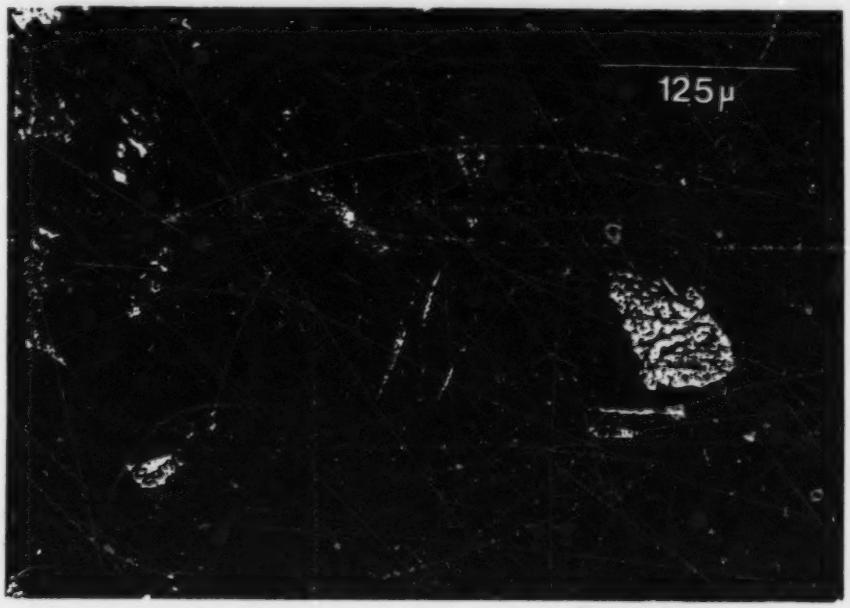

Photograph 6 - 200 X Reflected Light (Crossed Nicols)
Liberated particles of stibnite exhibit well developed wedge pressure twins, granular polygonal aggregates and untwinned to sector twinned individual crystals.

1036A

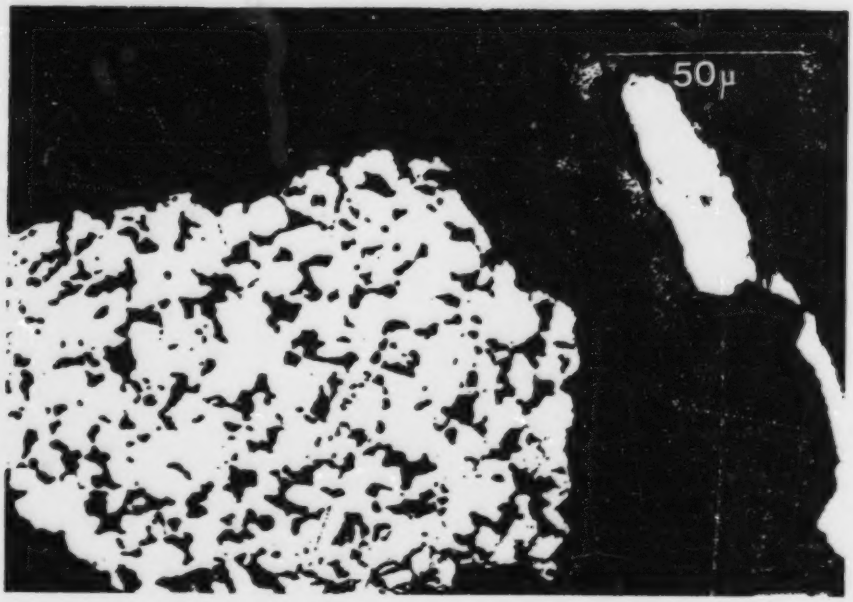

Photograph 7 - 500 X Reflected Light
Liberated aggregate of idiomorphic to xenomorphic native antimony. Also, binary association of subidiomorphic native antimony and pyrrhotite which exhibits high liberation potential at finer grind.

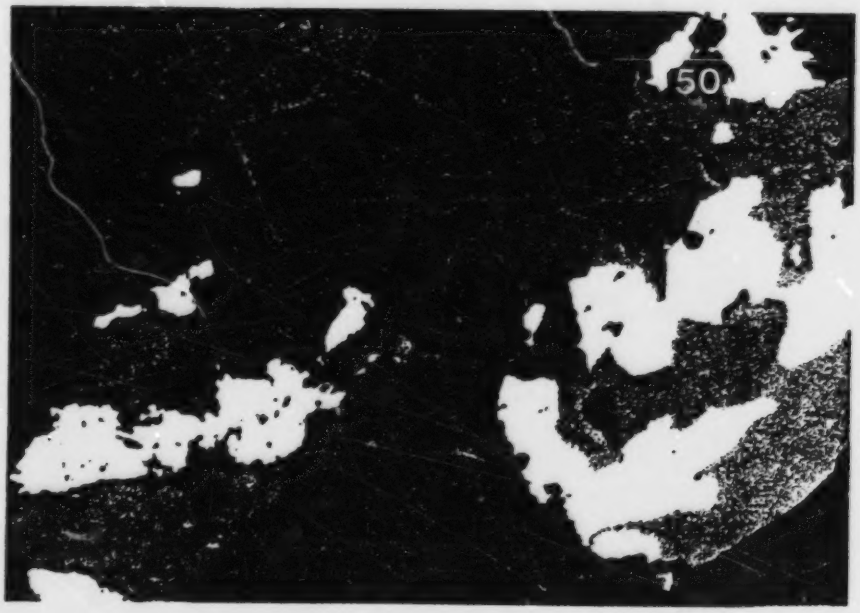

Photograph 8 - 500 X Reflected Light
Binary associations exhibiting high percentage liberation potential of (1) subidiomorphic to idiomorphic stibnite and minute crystals of native antimony in aggregates and (2) idiomorphic to xenomorphic native antimony cemented by pyrrhotite. Stibnite formed minute particles within native antimony and patchy relicts within pyrrhotite.

WD1

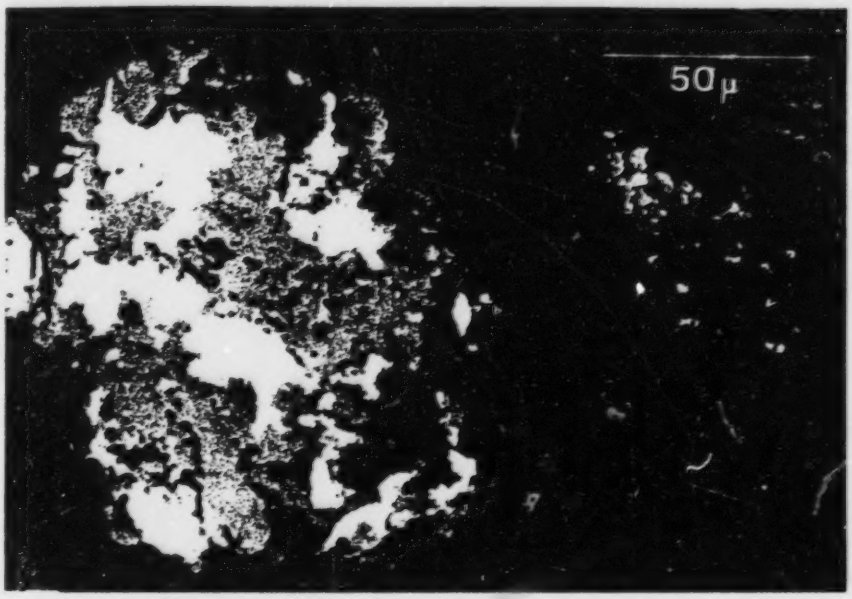

Photograph 9 - 500 X Reflected Light
Binary associations exhibiting fine particle size and difficult liberation potential of (1) native antimony -pyrrhotite and (2) stibnite-pyrite. Native antimony formed fine to coarse, idiomorphic to xenomorphic crystals cemented by and corroded by coarse to very fine interstitial pyrrhotite. Pyrite similarly forms fine granular particles cemented by stibnite.

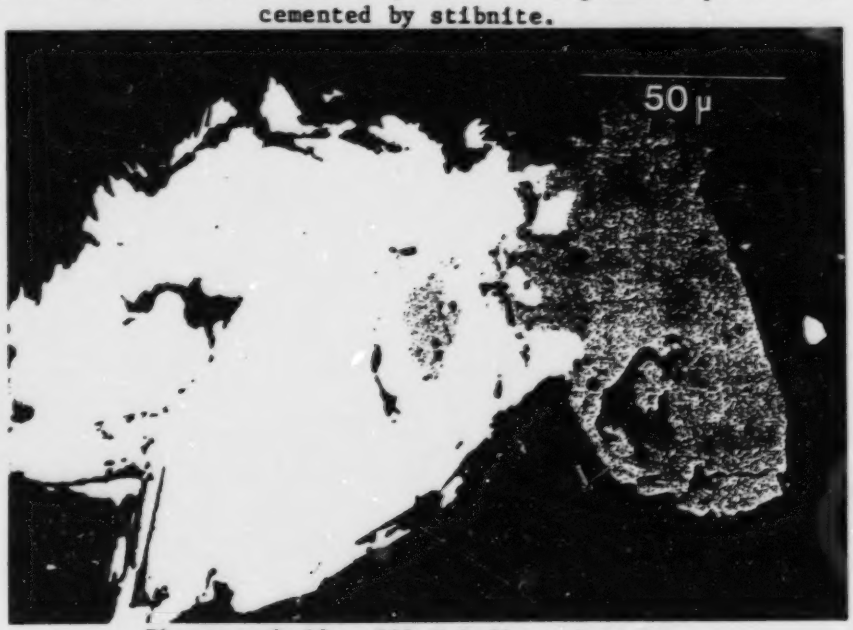

Photograph 10 - 500 X Reflected Light
Coarse binary association of native antimony and pyrrhotite exhibits fine interstitial cement penetration of native antimony by later pyrrhotite. Excellent to poor liberation characteristics.

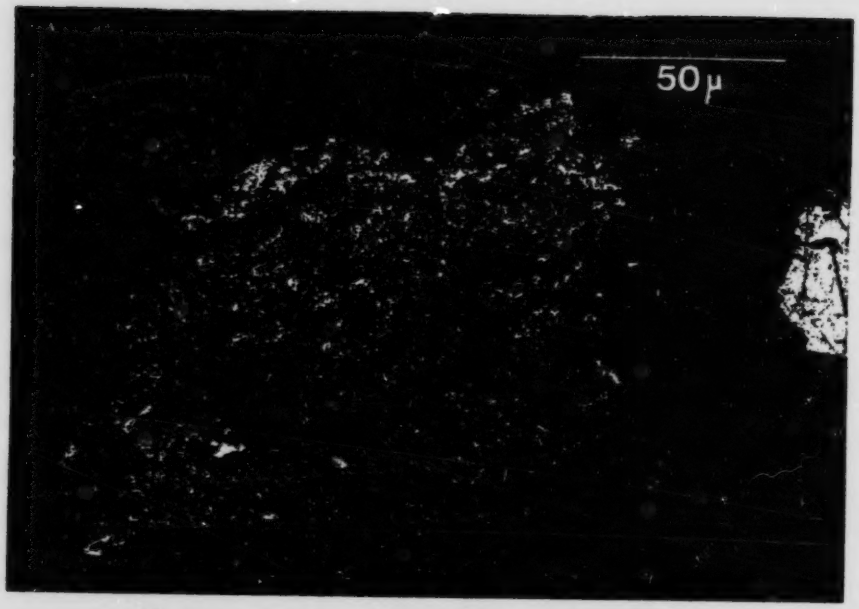

Photograph 11 - 500 X Reflected Light
Coarse liberated particle of pyrrhotite pseudomorphed after stibnite or berthierite.

Photograph 12 - 500 X Reflected Light
Polymineralic association of non-liberated native antimony enclosed by pyrrhotite and spatially associated to pyrite and arsenopyrite. The latter two minerals occur as discrete and binary grains cemented by pyrrhotite.

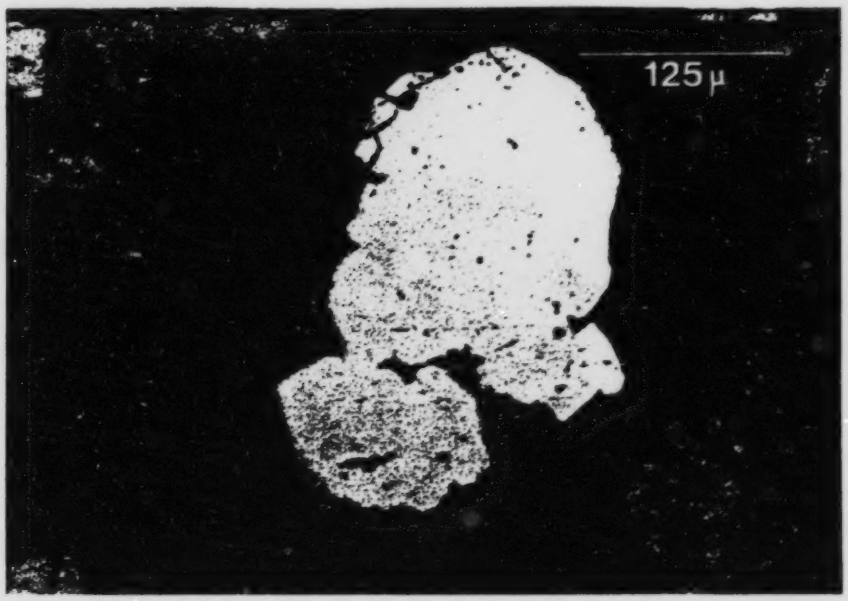

Photograph 13 - 200 X Reflected Light
Ternary (binary) association exhibiting concentrate dilution by stibnite cement over subidiomorphic pyrite-arsenopyrite aggregate.

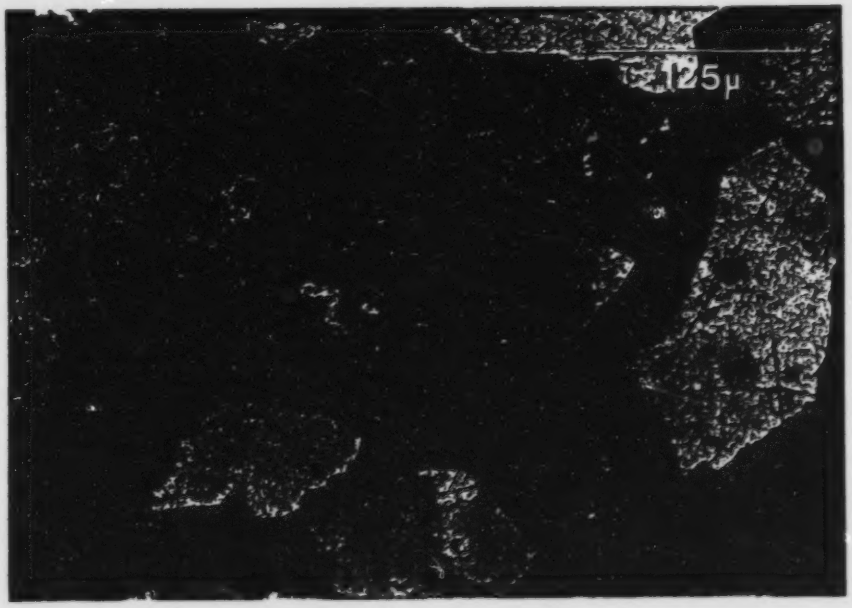

Photograph 14 - 200 X Reflected Light
Subidiomorphic crystals of silicate gangue are cemented by interstitial stibnite. Surface exposure of stibnite within gangue of less than 35%. Example of silicate dilution.

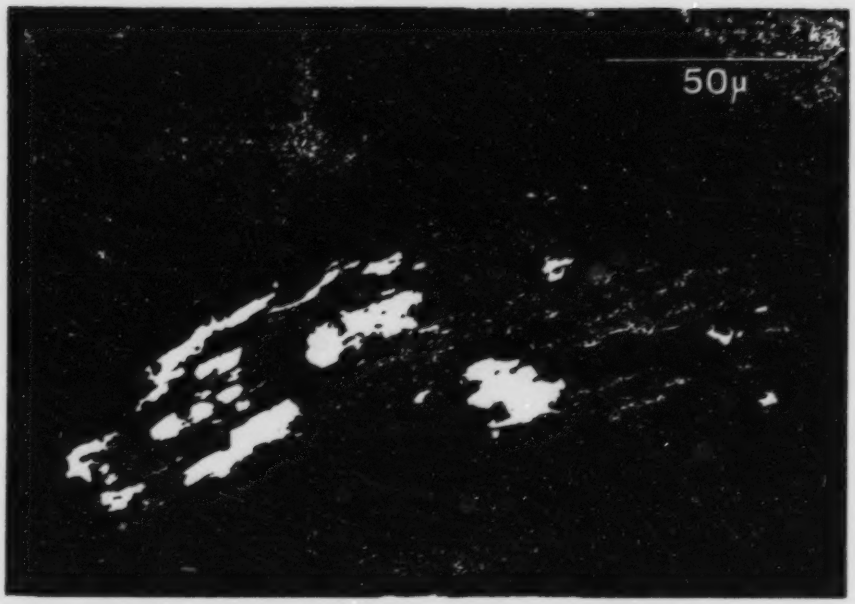

Photograph 15 - 500 X Reflected Light
Cleavage controlled replacement of silicates by stibnite and native antimony also exhibits poor liberation potential and dilution of concentrate product.

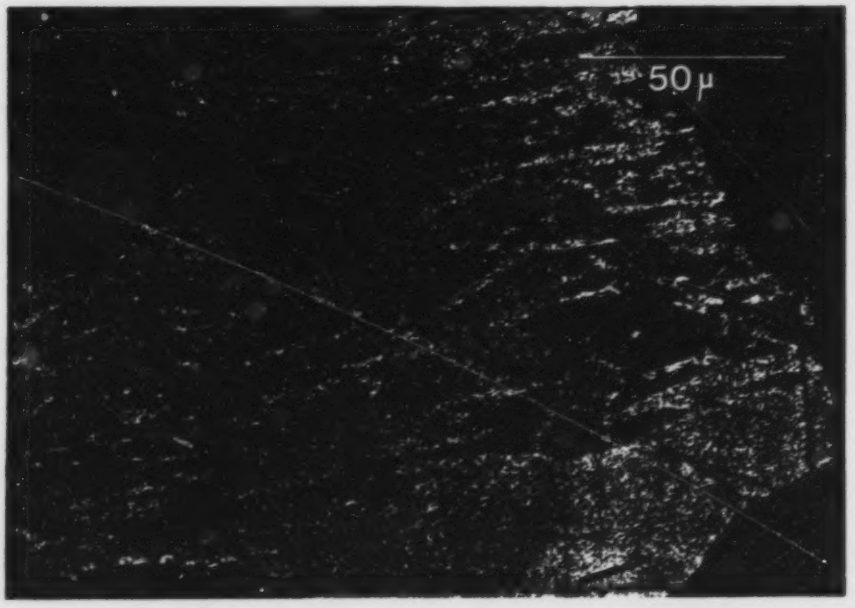

Photograph 16 - 500 X Reflected Light
Aggregate intergrowth of fine grained idiomorphic to locally xenomorphic stibnite and berthierite, the former typically prismatic and the latter primarily equant brown crystals. Interstitial silicate gangue exhibits moderate to poor liberation potential at finer grinds.

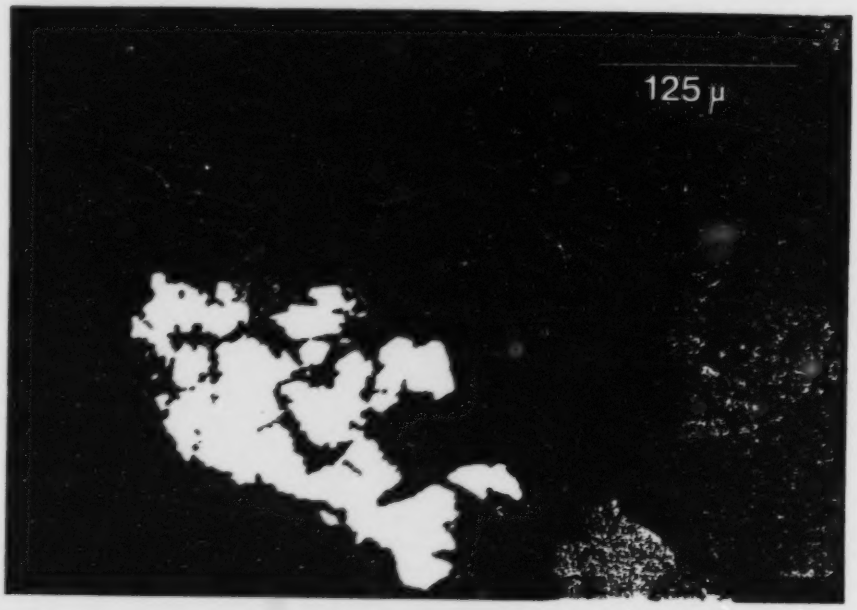

Photograph 17 - 200 X Reflected Light
Non-liberated association of silicate gangue enclosing coarse aggregate of idiomorphic to xenomorphic native antimony with later subidiomorphic chalcopyrite and prismatic stibnite. Excellent liberation potential of coarse native antimony with finer grind. Poor liberation expected from stibnite.

1036A

COARSE TAILINGS

Photograph 18 - 200 X Reflected Light
Coarse binary association of massive prismatic stibnite aggregate with minor fine-grained encapsulated stibnite. Minute xenomorphic crystals of native antimony are disseminated within the stibnite. High liberation potential with increased grinding.

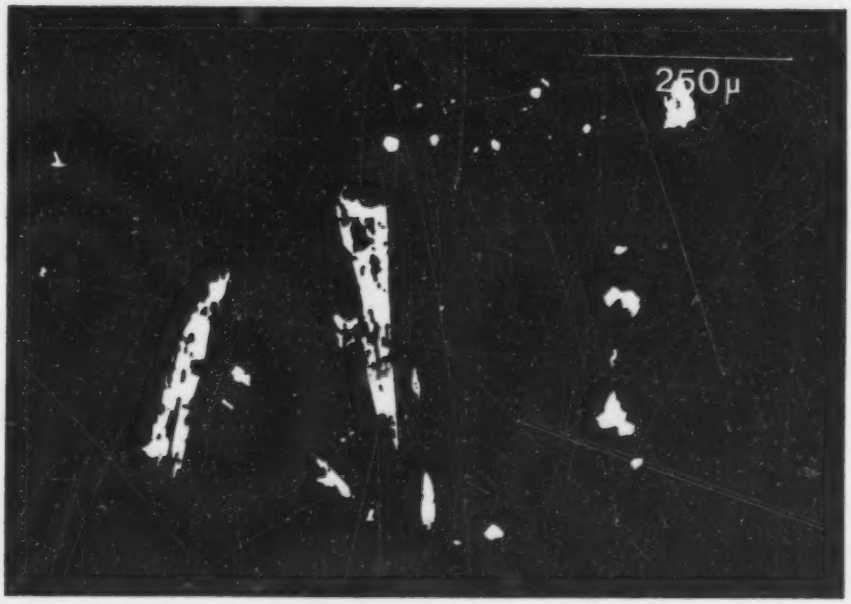

Photograph 19 - 100 X Reflected Light
Angular to subrounded silicate gangue particles contain minute to coarse, subidiomorphic to xenomorphic crystals of stibnite and native antimony. Coarse stibnite locally exhibits minor surface exposure in binary association. Liberation enhanced by further grinding.

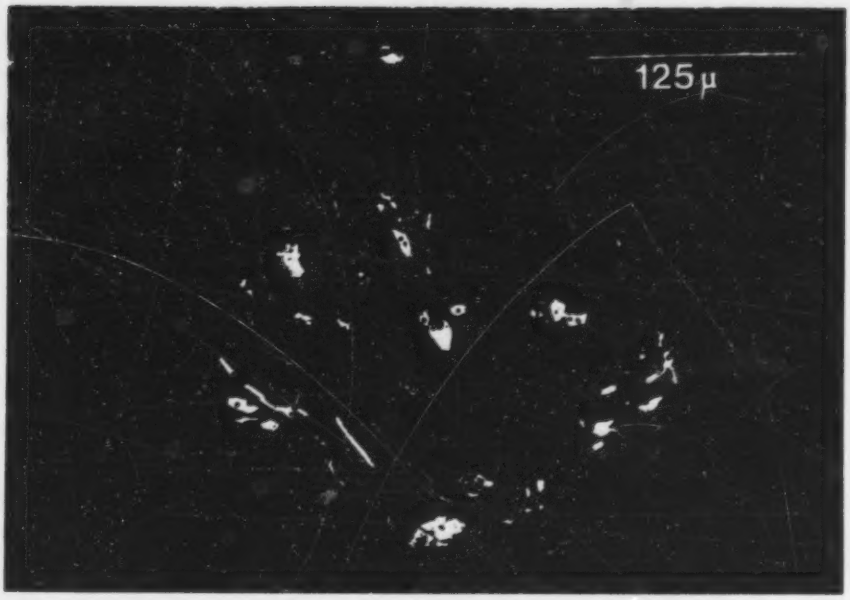

Photograph 20 - 200 X Reflected Light
Minute prismatic to equant, idiomorphic to xenomorphic stibnite and lesser native antimony encapsulated by silicate gangue. Liberation potential by further grinding poor to moderate.

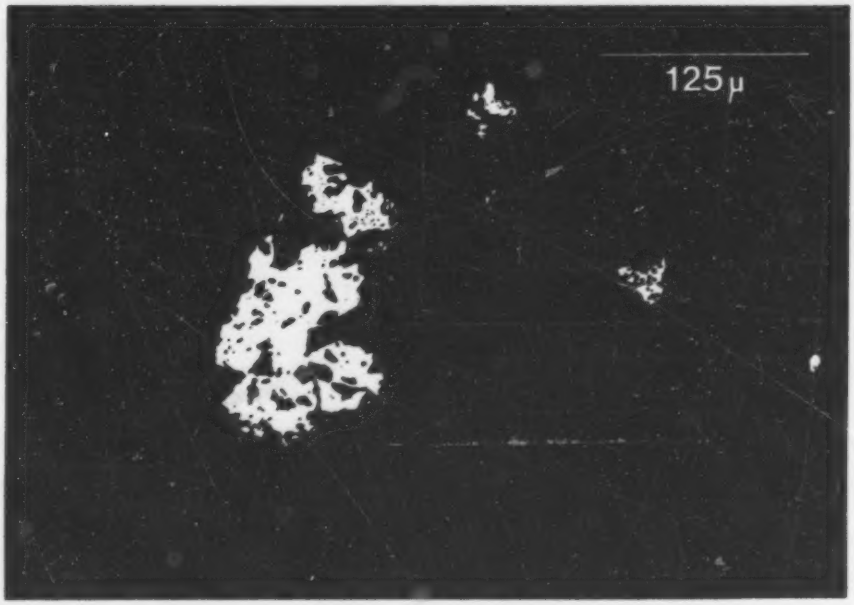

Photograph 21 - 200 X Reflected Light
Non-liberation exhibited by interstitial stibnite enclosed by silicate gangue, also by equant, subidiomorphic stibnite and native antimony in middling association with pyrrhotite and silicate gangue.

1036A

FINE FEED

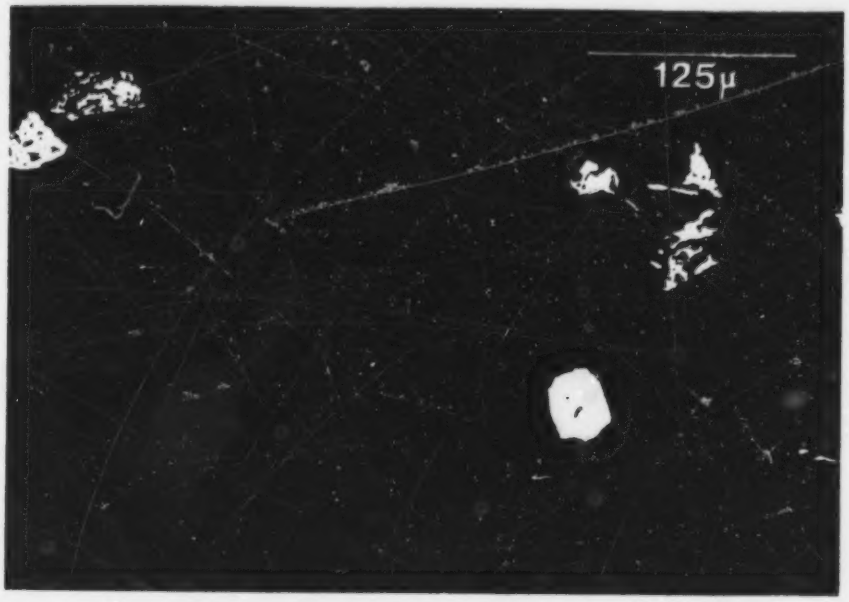

Photograph 22 - 200 X Reflected Light
Overview of liberated and encapsulated stibnite within silicates, also diluents pyrite, pyrrhotite and silicates. Very fine stibnite locked within silicate will report to tailings product.

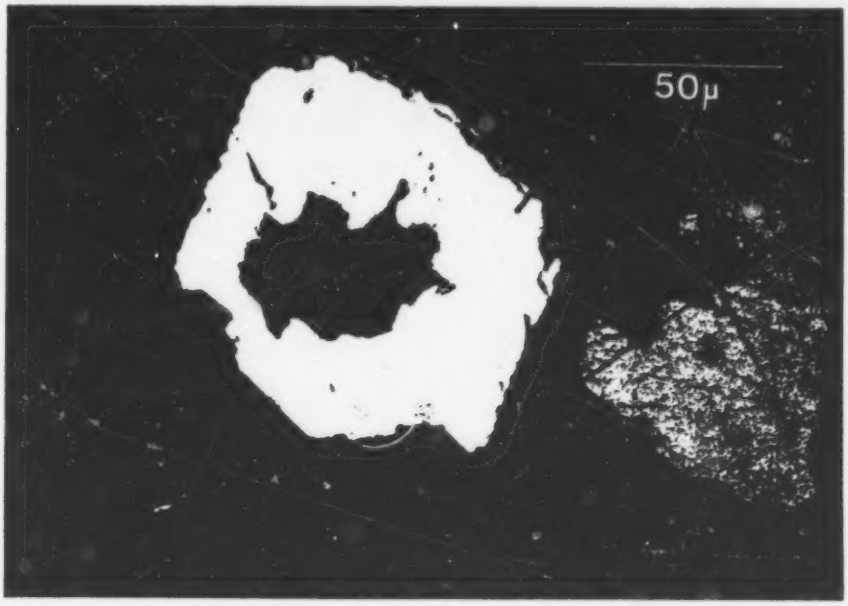

Photograph 23 - 500 X Reflected Light
Liberated subidiomorphic to xenomorphic angular particles of stibnite and also native antimony-stibnite binary. The antimony encloses both stibnite and minor pyrite.

1036A

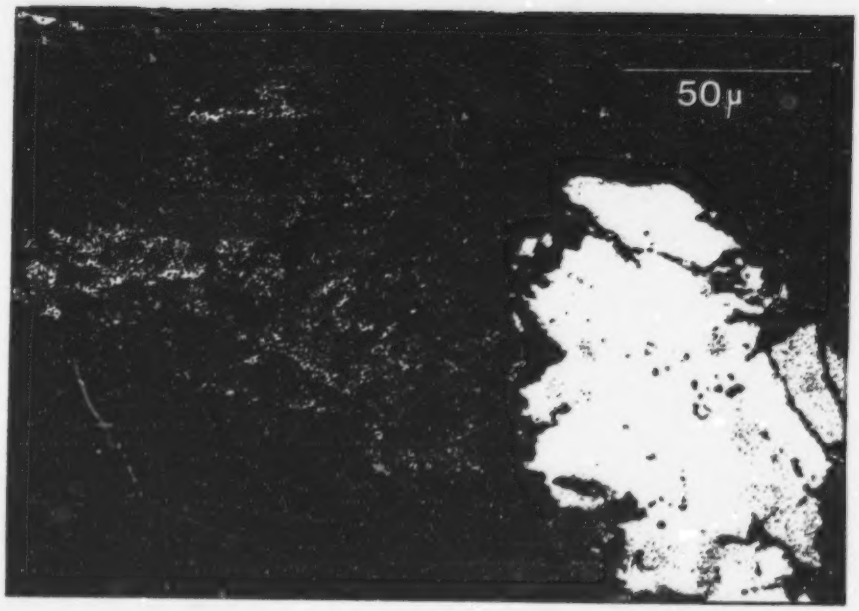

Photograph 24 - 500 X Reflected Light
Binary association of stibnite-berthierite, typically as subequant to prismatic crystals attached to myrmekitic pyrite-arsenopyrite intergrowth. Silicate gangue occurred interstitial to the stibnite-berthierite prisms. Additional grinding required for liberation, though should report to concentrate.

1036A

WD1

FINE CONCENTRATE

Photograph 25 - 500 X Reflected Light
Overview of concentrate product exhibits abundant, liberated, angular to subidiomorphic stibnite crystals and aggregates, with lesser free particles of native antimony, and binary associations of stibnite or native antimony with unwanted pyrrhotite diluent. Binary associations between stibnite and silicate gangue were also observed.

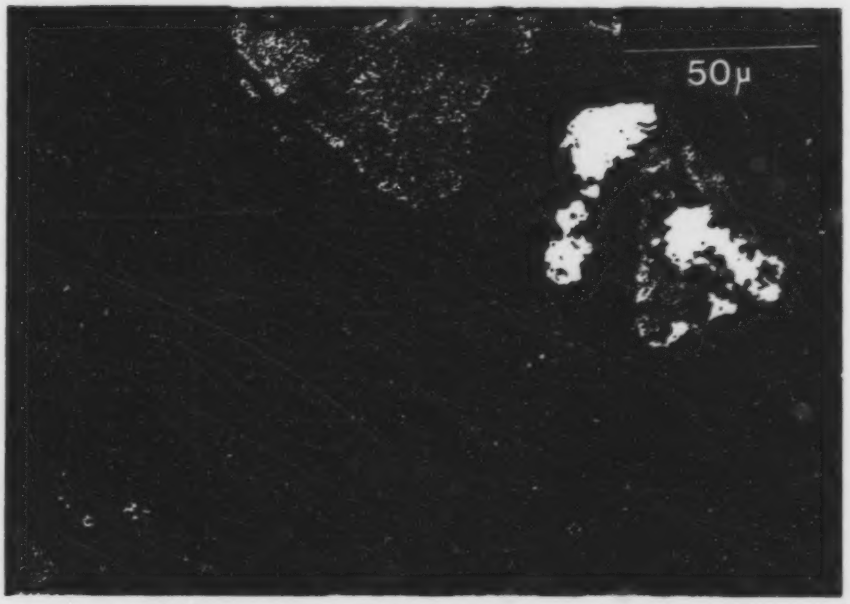

Photograph 26 - 500 X Reflected Light
Native antimony occurs as xenomorphic liberated grain aggregates and complex binary intergrowths with pyrrhotite. Stibnite occurs primarily as liberated massive particles and also with native antimony as porous coatings around silicate gangue. The association represents interstitial stibnite after silicates in the ore paragenesis.

Photograph 27 - 500 X Reflected Light
Coarse ternary association between stibnite, chalcopyrite and silicate gangue. Liberation achieved by fine grind though complete liberation only at ultrafine grinds.

Photograph 28 - 500 X Reflected Light
Ternary association of native antimony, stibnite, and pyrrhotite. The pyrrhotite forms replacement after early stibnite which encapsulated native antimony. Complete liberation difficult.

1036A

FINE TAILINGS

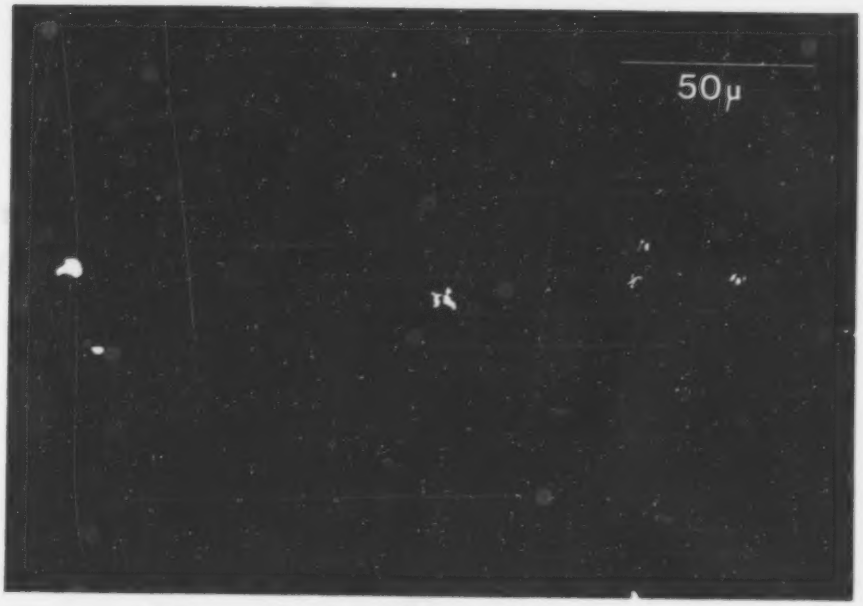

Photograph 29 - 500 X Reflected Light
Overview of flotation tailings exhibits only minor stibnite and native antimony in middling or binary associations with silicate gangue.

1036A

ULTRAFINE FEED

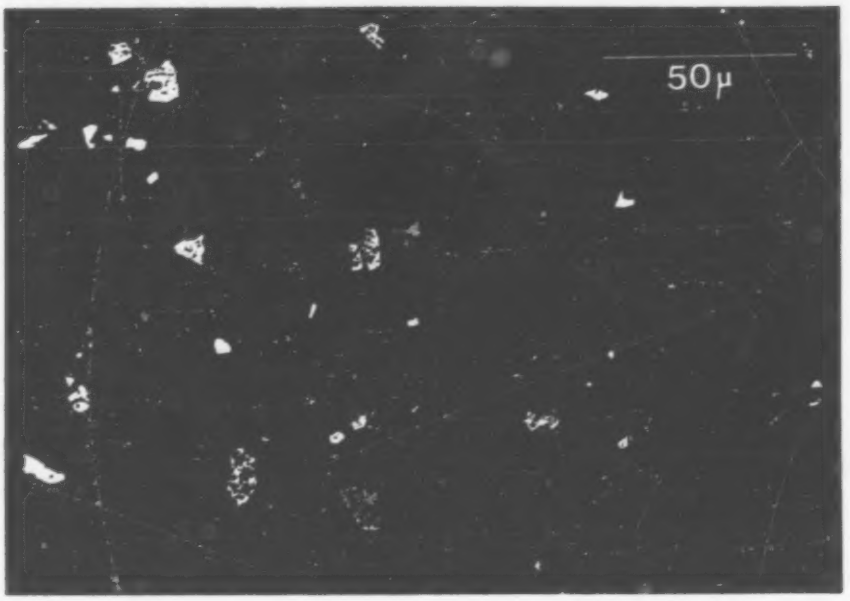

Photograph 30 - 500 X Reflected Light
Overview of ultrafine grind exhibits high percentage of liberated stibnite (berthierite) and lesser particles of native antimony, locally as binary associations with stibnite.

1036A

ULTRAFINE CONCENTRATE

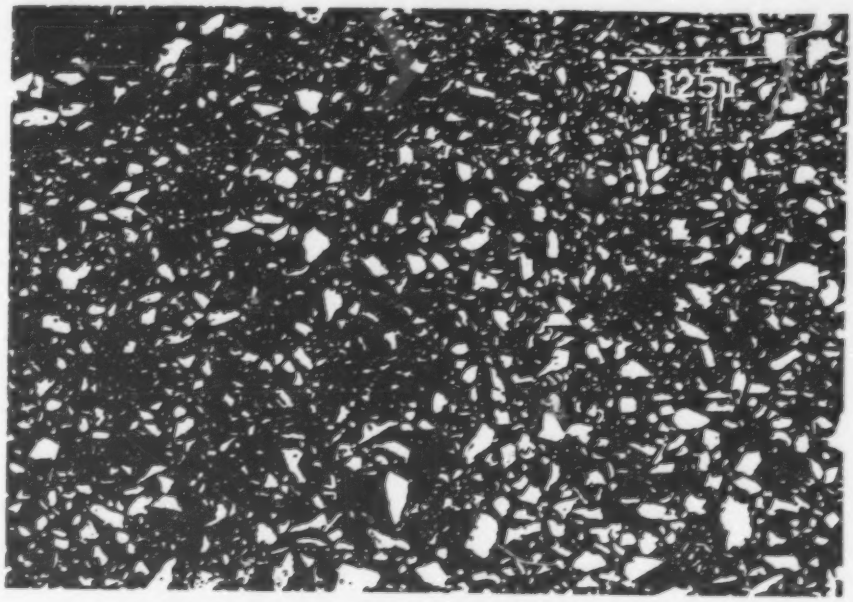

Photograph 31 - 200 X Reflected Light
Overview of antimony concentrate exhibits high percentage of liberated stibnite (berthierite) and lesser native antimony, the latter as free and binary associations (stibnite).

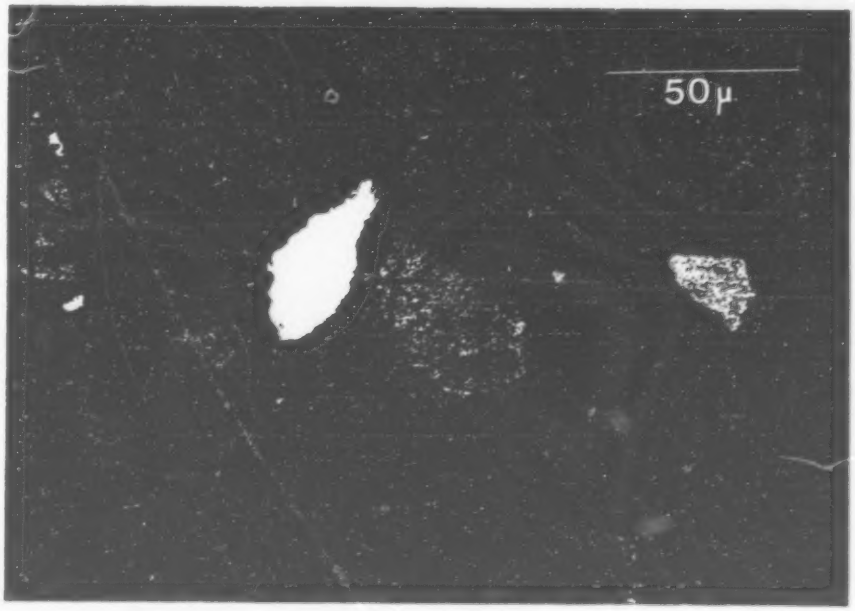

Photograph 32 - 500 X Reflected Light
Angular liberated fragments of stibnite and binary association of stibnite-native antimony. Liberated diluent particles of pyrite and pyrrhotite are also observed.

ULTRAFINE TAILINGS

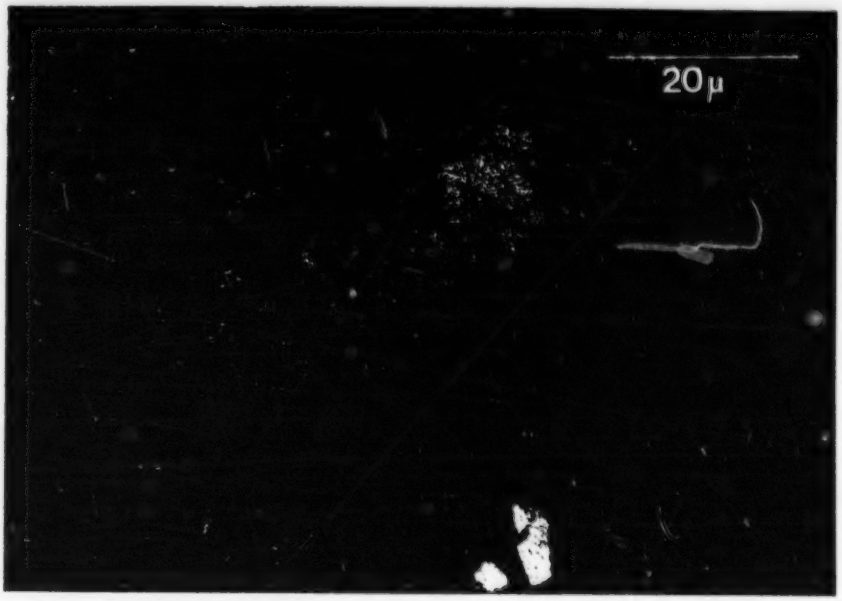

Photograph 33 - 1250 X Reflected Light (oil immersion)
Liberated prism of stibnite in ultrafine flotation tailings.

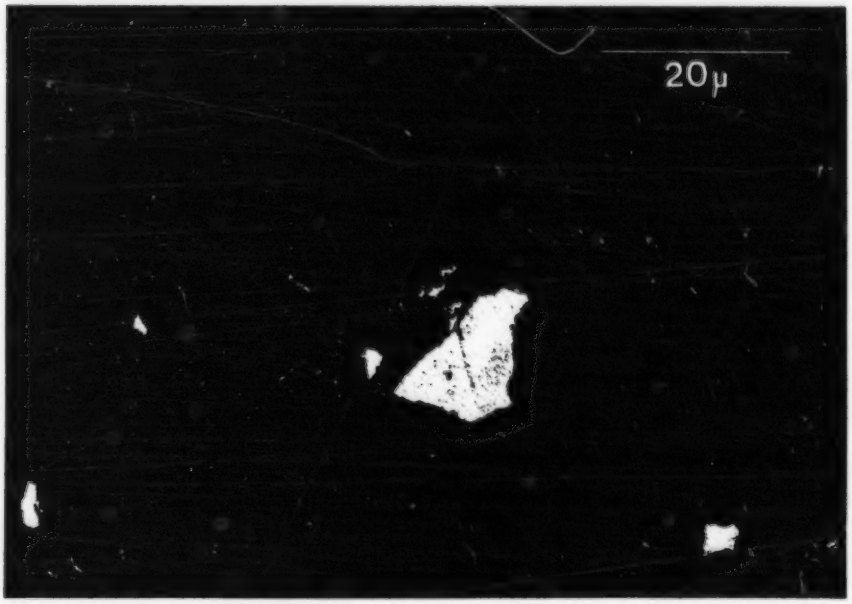

Photograph 34 - 1250 X Reflected Light (oil immersion)
Binary association of stibnite-pyrite in ultrafine flotation tailings.

1036A